Plant Stress 12 (2024) 100428

Contents lists available at ScienceDirect

Plant Stress

journal homepage: www.sciencedirect.com/journal/plant-stress

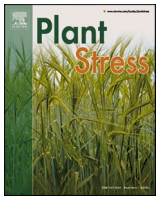

# Nutrient flow environment as a eustress that promotes root growth by regulating phytohormone synthesis and signal transduction in hydroponics

Bateer Baiyin [a], Yue Xiang [a], Yang Shao [b], Jiangtao Hu [a], Jung Eek Son [c], Kotaro Tagawa [d], Satoshi Yamada [d], Qichang Yang [a,*]

[a] Research Center for Smart Horticulture Engineering, Institute of Urban Agriculture, Chinese Academy of Agricultural Sciences, Chengdu National Agricultural Science & Technology Center, Chengdu 610213, China
[b] National Key Laboratory of Crop Genetic Improvement, College of Plant Science & Technology, Huazhong Agricultural University, Wuhan 430070, China
[c] Department of Agriculture, Forestry and Bioresources, Seoul National University, Seoul 08826, Republic of Korea
[d] Faculty of Agriculture, Tottori University, Tottori 680-8553, Japan

ARTICLE INFO

*Keywords:*
Root morphology
Plant hormone
Nutrient solution flow environment
Transcriptome
Hydroponics
Urban agriculture

ABSTRACT

The morphology of lettuce roots in hydroponics is affected by the flow environment of nutrient solutions. Regulating the flow rate therefore ensures quality and yield; however, the mechanisms underlying this impact have not been fully elucidated, and breakthroughs in regulatory methods are thus lacking. Herein, lettuce was grown in a hydroponic solution at three different flow rates, the root morphology indicators (such as root length and surface area) were evaluated, the hormone levels of roots grown under different flow conditions were measured, and the correlations between plant hormones and root morphology were analyzed. Transcriptomic analysis was conducted on roots at varying flow rates to investigate the differential expression of genes involved in the synthesis and signal transduction pathways of auxin, abscisic acid (ABA), ethylene, and jasmonic acid. Results showed that these plant hormones were closely related to root morphology. Compared to a non-flow environment, a flow environment promoted the synthesis of plant hormones in the roots and enhanced the signal transduction of certain hormones, such as auxin. However, it had a negative impact on the signal transduction of certain hormones, specifically ethylene. The flow of the nutrients regulated root morphogenesis by influencing the synthesis and transduction of plant hormones, which affected overall plant growth. During the same growth period, lettuce grown under suitable flow conditions had a higher fresh weight than lettuce grown under no-flow conditions. Although such flow would increase the electricity cost of operating water pumps, lettuce could be harvested in advance at appropriate flow rates, thereby reducing the energy consumed in plant factories through lighting and temperature regulation, which are the largest contributors to energy consumption. This study examined the impact of the nutrient solution flow environment as a positive stimulus for plant growth, and it provides a reference for strategically regulating the flow rate in plant factories to improve yield and save energy. Future research should explore the effects of other cultivation and flow methods on the growth of different plants and apply these findings to practical production.

*Abbreviations:* 13-HPOT, 13-hydroperoxyoctadecatrienoic acid; ABA, abscisic acid; ACC, 1-aminocyclopropane-1-carboxylic acid; ACS, ACC synthase; ACO, ACC oxidase; ARF, auxin response factor; BHLH, basic helix loop helix; BP, biological processes; CC, cellular component; CE, collision energy; COG, clusters of orthologous groups; COI1, coronatine insensitive 1; CUR, curtain gas; DP, declustering potential; ETR, ethylene receptor 2; GO, Gene Ontology; IAA, indole acetic acid; IS, ion spray; JA, jasmonic acid; JAZ, jasmonate ZIM; JMT, jasmonic acid carboxyl methyltransferase; LIT, linear ion trap scan; MF, molecular function; MRM, multiple reaction monitoring; MSE, mean ± standard error; MVA, mevalonate; OPDA, 12-oxo phytodienoic acid; PCA, principal component analysis; PEG, photosynthetic photon flux density; PPFD, polyethylene glycol; PP2C, protein phosphatase 2C; PYL, pyrabactin-like; PYR, pyrabactin resistance; QQQ, triple quadrupole scan; SAM, S-adenosylmethionine; SnRK2, sucrose non-fermenting 1-related protein kinase 2; XAN, xanthaldehyde.

* Corresponding author.
*E-mail address:* yangqichang@caas.cn (Q. Yang).

https://doi.org/10.1016/j.stress.2024.100428
Received 12 January 2024; Received in revised form 27 February 2024; Accepted 7 March 2024
Available online 16 March 2024

## Introduction

Hydroponics is a modern cultivation technology that uses nutrient solutions instead of soil and is used to grow various plant species, including vegetables, herbs, and flowers (Sheikh, 2006). It is a resource-efficient method that achieves high yields and efficiency, thereby providing a sustainable solution to crop production to meet the fresh and organic agricultural product demands of urban populations and playing a key role in urban and vertical agriculture (Mir et al., 2022).

Hydroponics involves the use of a fluid nutrient solution as a growing medium (Baiyin et al., 2021a). It is a controlled environmental agriculture practice in which the growing conditions, particularly the root environment, are artificially controlled to support plant growth. The quality and yield of crops are therefore directly affected by the suitability of the hydroponic root environment (Li et al., 2018). Since the introduction of hydroponics, researchers have extensively studied the effect of the root environment on plant growth, and most have focused on the effects of the nutrient solution composition (Kang and Kim, 2007), concentration (Sakamoto and Suzuki, 2020), pH (Gillespie et al., 2020), temperature (Thakulla et al., 2021), and other growth indicators. Plant growth in hydroponics is affected by the nutrient flow solution, and this has received greater research attention than other environmental indicators. For example, Al-Tawaha et al. (2018) investigated the effects of three nutrient solution flow rates on lettuce growth and reported that 20 L/min increased the fresh weight of lettuce. Soares et al. (2020) assessed the effects of different nutrient solution flow rates on vegetable production and found that a flow rate of 1.5 L/min was the most effective for increasing stem fresh weight, dry weight, leaf area, leaf number, plant height, and stem diameter. Baiyin et al. (2021a) conducted used five flow rate conditions when growing Swiss chard and found that a flow rate of 6 L/min provided the highest plant fresh weight. The study also observed significant differences in root morphology, including root length and surface area, among different flow rates (Baiyin et al., 2021a).

As root morphology is a crucial indicator of plant growth and nutrient uptake, optimizing the flow rate can improve root morphology, nutrient uptake, and nutrient use efficiency (Baiyin et al., 2021b). The response of root morphology to environmental conditions is closely linked to phytohormone action (Vissenberg et al., 2020). Phytohormones regulate and facilitate adaptive responses when roots experience stress or unfavorable environmental conditions. Through interaction and coordination, hormones regulate root development and morphogenesis, ensuring root health and adaptability to the environment (Pacifici et al., 2015). Auxins, a type of phytohormone, are crucial for root morphology (Saini et al., 2013); they stimulate root cell elongation and promote root hair growth. Ethylene, another phytohormone, has multiple effects on root morphology (Vandenbussche et al., 2012), stimulating root elongation and fine root formation and participating in lateral root differentiation. Jasmonate functions as a signaling molecule and is crucial for root morphology development (Huang et al., 2017), promoting root hair and lateral root growth, which increases the absorptive surface area and water uptake capacity. Furthermore, ABA plays an important regulatory role in root morphology (Hong et al., 2013) as it hinders the formation of lateral roots and contributes to the root stress response. All four (auxins, ethylene, jasmonate, and ABA) regulate root development and morphogenesis in response to environmental conditions; their actions overlap and differ in relation to various biological processes, enabling plants to maintain healthy root systems and adapt to their environment.

Previous studies on the relationship between hormones and root morphology have primarily been based when cultivating plants in soil or substrate. Although the rhizosphere environment and hydroponics differ significantly from soil and substrate cultivation due to the lack of media flow, the effects of hormones on root morphology in hydroponic systems have not been substantially studied. It is therefore necessary to explore how the physical environment of the nutrient solution flow in hydroponics affects hormone synthesis and transduction, root morphology, and crop production. Investigating the influence of nutrient solution flow on phytohormones in hydroponics can be challenging due to the unique cultivation environment

We hypothesized that the flow rate of the hydroponic nutrient solution can regulate the formation of root morphology by controlling the synthesis and transduction of phytohormones, thus influencing crop production. To test this hypothesis, hydroponic lettuce cultivation was conducted at different flow rates, and differences in the morphology, phytohormone concentrations, and key gene transcript levels in roots were examined. In this context, it was important to investigate the mechanisms by which the flow of nutrient solution in hydroponics controlled the root morphology and its effects on crop production. These findings contribute to optimizing hydroponic cultivation conditions and improving crop yield and quality.

## Materials and methods

### *Planting methods and cultivation conditions*

Lettuce seeds ("Italian fast growing" variety, sourced from Long tillage, Hebei Manchou Agri-Tech Co., Ltd) were sown in a seedling tray filled with moist vermiculite. After seven days, the seedlings were carefully transplanted into plastic containers filled with a standard concentration nutrient solution for an additional seven days without flow rate.

Subsequently, the plants were transferred to cultivation tanks (dimensions: 1.7 m length, 0.2 m width, and 0.2 m height). At this stage, flow rate treatment was conducted. Each tank was filled with 50 liters of the same standard concentration nutrient solution at a pH of 5.8 and an electrical conductivity of 2.30. The specific components and concentrations of the nutrient solution (vegetable & flower general nutrient solution, provided by Caijudongli Agri-Tech Co., Ltd) are detailed in Table 1.

The experiment was designed with three different flow rate treatments: F0 (0 L/min), F7 (7 L/min), and F14 (14 L/min). Each treatment had four replicates, consisting of four cultivation tanks with five plants each. The nutrient solution flow was controlled using a water pump (Model XDP-7500, Sensen Group Co., Ltd) and monitored with a flow meter (Model ZJ-LCD-S2, Sensor B7, both from Zhongjiang Dianzi Co., Ltd). Illumination was provided by an LED light (Model WZ-90, Shandong Guixiang Guangdian Co., Ltd) set to a 14:10 hour light:dark cycle. Light intensity on the cultivation board was measured using a photometry instrument (AvaSpec-ULS2048XL-RS-EVO, Avantes), maintaining a photosynthetic photon flux density (PPFD) of approximately 550 μmol/$m^2$s. Detailed spectral information of the light source is presented in Fig. 1B. Throughout the cultivation period, the ambient temperature in the room was maintained at 25 ± 1 °C, with a relative humidity of 65 ± 5 %.

The experiment was designed to minimize the influence of

**Table 1**
Composition and concentration of the standard nutrient solution employed (Baiyin et al., 2023).

| Composition | Concentration (mg/L) |
|---|---|
| $Ca(NO_3)_2{\cdot}4H_2O$ | 945 |
| $KNO_3$ | 607 |
| $NH_4H_2PO_4$ | 115 |
| $MgSO_4{\cdot}7H_2O$ | 493 |
| $Na_2Fe(EDTA)$ | 20–40 |
| $H_3BO_3$ | 2.86 |
| $MnSO_4{\cdot}4H_2O$ | 2.13 |
| $ZnSO_4{\cdot}7H_2O$ | 0.22 |
| $CuSO_4{\cdot}5H_2O$ | 0.08 |
| $(NH_4)_6Mo_7O_{24}{\cdot}4H_2O$ | 0.02 |

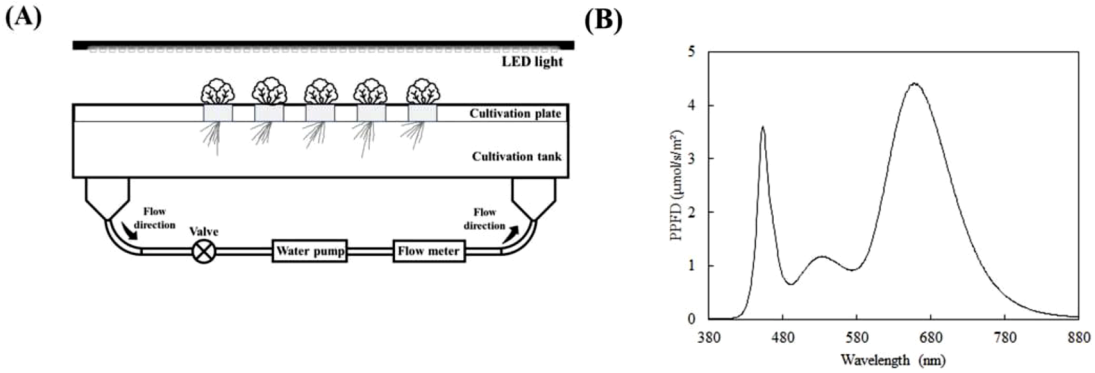


**Fig. 1.** Schematic diagram of (A) cultivation device, and (B) LED light spectrum (Baiyin et al., 2023).

extraneous environmental factors, ensuring that the observed effects were solely attributable to the nutrient solution flow environment's impact on root morphology. Notably, an increase in flow rate is known to elevate dissolved oxygen levels in water. This effect occurs due to the disruption of the water–air interface, enhancing the mixing and contact between oxygen and water molecules, which in turn improves oxygen solubility (Baiyin et al., 2021c). Therefore, we used covered cultivation boards to isolate the water–air interface and prevent any impact from the increased oxygen content caused by the flow, thereby avoiding any additional effects of the flow.

### *Determination of root morphology*

On the 14th day post-planting, we proceeded with the sampling of the plants subjected to varying flow rates. The shoots and roots were carefully separated for further analysis. Root morphology parameters, including total root length, root surface area, root volume, and average root diameter, were quantified using a root scanner coupled with WinRhizo 2013 software (Regent Instruments Inc., Quebec, QC, Canada).

The fresh weight of the samples was determined using an electronic balance (Model FA2204, Shanghai Lichen Co., Ltd). For detailed analysis of plant hormone content and transcriptome sequencing, root samples were immediately frozen in liquid nitrogen for 15 min and subsequently stored at −80 °C.

### *Determination of plant hormones*

#### *Sample preparation and extraction*

For the analysis of lettuce root samples, they were first removed from storage at −80 °C and ground into a fine powder using a grinder (Model MM 400, Retsch) at 30 Hz for 1 min. Fifty milligrams of the powdered sample was then placed into a 2 mL plastic microtube and quickly frozen in liquid nitrogen. This was followed by dissolving the sample in 1 mL of a methanol/water/formic acid mixture (15:4:1 v/v/v).

To the dissolved sample, 10 microliters of an internal standard solution (100 ng/mL) was added for quantification purposes. The mixture was then vortexed for 10 min and subsequently centrifuged at 11,304 × *g* for 5 min at 4 °C. The supernatant was transferred to a new plastic microtube and evaporated to dryness. The dry residue was reconstituted in 100 μL of 80 % methanol (v/v) and passed through a 0.22 μm membrane filter in preparation for LC-MS/MS analysis, as described by Floková et al. (2014). This procedure was replicated across four biological samples.

#### *UPLC conditions*

The sample extracts were analyzed using an UPLC-ESI-MS/MS system, comprising an ExionLC™ AD UPLC unit and a QTRAP® 6500+ mass spectrometer (both from SCIEX, https://sciex.com.cn/). The analytical conditions were set as follows: the column used was a Waters Acquity UPLC HSS T3 C18 (100 mm × 2.1 mm i.d., 1.8 μm). The solvent system consisted of water with 0.04 % acetic acid (Solvent A) and acetonitrile with 0.04 % acetic acid (Solvent B). The gradient program began at 5 % B for 0–1 min, increased linearly to 95 % B over 1–8 min, held at 95 % B for 8–9 min, and then returned to 5 % B from 9.1 to 12 min. The flow rate was maintained at 0.35 mL/min, with a column temperature of 40 °C. Each injection volume was 2 μL, as per the method described by Xiao et al. (2018).

#### *ESI-MS/MS conditions*

Phytohormone analysis was conducted using a QTRAP® 6500+ LC-MS/MS System equipped with an ESI turbo ion spray interface, capable of both Linear ion trap (LIT) and triple quadrupole (QQQ) scans. This system, controlled by Analyst 1.6.3 software (Sciex), operated in both positive and negative ion modes. The ESI source operation parameters were set as follows: ion source ESI+/-; source temperature at 550 °C; ion spray voltage (IS) at 5500 V in positive and −4500 V in negative mode; and curtain gas (CUR) at 35 psi.

Scheduled multiple reaction monitoring (MRM) was employed for phytohormone analysis. Data acquisition and subsequent analysis were performed using Analyst 1.6.3 and Multiquant 3.0.3 software (Sciex), respectively. The mass spectrometry parameters, including declustering potential (DP) and collision energy (CE) for individual MRM transitions, underwent further optimization. We monitored a specific set of MRM transitions tailored to each period based on the metabolites eluted, as detailed in the method by Šimura et al. (2018).

### *RNA extraction, library construction, and sequencing*

RNA sequencing was performed on twelve samples representing three flow rates (F0, F7, and F14), with four biological replicates each. RNA extraction followed the CTAB method. Approximately 100 mg of ground sample was mixed with 1 mL of CTAB solution and incubated at 60 °C for 10 min. Post incubation, the sample was centrifuged for 5 min at 12,000 × *g*. The supernatant was then extracted with an equal volume of chloroform, mixed, and centrifuged twice, each time for 5 min at 12,000 × *g*. The resulting supernatant was mixed with an equal volume of LiCl and left to stand for 2 h at −20 °C, followed by centrifugation for 20 min at 12,000 × *g*. The pellet was washed with 75 % ethanol, centrifuged for 5 min at 12,000 × g, and allowed to stand at room temperature for 5 min. The RNA was then resuspended in 30 μL of DEPC-treated water and stored at −80 °C.

RNA quality was assessed at multiple stages: degradation and contamination were checked using 1 % agarose gel electrophoresis; purity was verified using a NanoPhotometer (IMPLEN, CA, USA); concentration was measured with the Qubit RNA Assay Kit on a Qubit 2.0 Fluorometer (Life Technologies, CA, USA); and integrity was assessed using an RNA Nano 6000 Assay Kit on a Bioanalyzer 2100 system

(Agilent Technologies, CA, USA).

The cDNA libraries for lettuce roots were prepared as described by Chen et al. (2016). These libraries were then sequenced on an Illumina NovaSeq 6000 platform to generate 150-bp paired-end reads.

*Read mapping and differentially expressed gene analysis*

For RNA-seq data processing, Fastp (Chen et al., 2018) was utilized to filter out adapter sequences and remove reads. Paired reads were removed if the proportion of unidentified nucleotides (N) exceeded 10 % or if low-quality bases (Q20) constituted over 50 % of the reads. The resulting clean reads were aligned with the *Lactuca sativa* reference genome (available at https://ftp.ncbi.nlm.nih.gov/genomes/all/GCF/002/870/075/GCF_002870075.3_Lsat_Salinas_v8) using HISAT2 (http://ccb.jhu.edu/software/hisat2/index.shtml) (Kim et al., 2015).

Gene alignment counts were generated using featureCounts (Liao et al., 2014), and the fragments per kilobase of exon per million fragments mapped (FPKM) for each gene were calculated, accounting for variations in gene length and sequencing depth. Differential gene expression analysis between groups was conducted using DESeq2 (Love et al., 2014), with the P-value adjusted using the Benjamini and Hochberg method for controlling the false discovery rate (FDR). Genes were considered differentially expressed (DEGs) if they met the criteria of an FDR $< 0.05$ and an absolute log2Fold Change of $\geq 1$.

*Differential gene annotation and enrichment analysis*

Gene function enrichment analysis for the differentially expressed genes (DEGs) was conducted using the Gene Ontology (GO) and Kyoto Encyclopedia of Genes and Genomes (KEGG) databases. Specifically, the DEGs identified in the transcriptomes were annotated using a BLAST search. This annotation involved a comprehensive search against several protein databases, including KEGG, the NCBI non-redundant sequence (NCBI NR) database, the Clusters of Orthologous Groups of proteins (COG), and the Swiss-Prot database, maintained by the Swiss Institute of Bioinformatics.

*Quantitative real-time PCR validation*

To validate the RNA-Seq findings, we selected 16 DEGs associated with plant hormone synthesis and transduction for qRT-PCR analysis. The same RNA samples were reverse-transcribed into cDNA using the PrimeScript TM 1st Strand cDNA Synthesis Kit. qRT-PCR amplifications were carried out in a Roche LightCycler 480 II. The PCR conditions included an initial denaturation at 95 °C for 5 min, followed by 40 cycles of 95 °C for 15 s for denaturation, and 60 °C for 30 s for annealing and extension. The relative expression levels of the genes were quantified using the $2^{-\Delta\Delta CT}$ method, as outlined by Livak and Schmittgen (2001). Each sample was analyzed in triplicate to ensure technical accuracy. The specific primers employed in this study are detailed in Table S1.

*Statistical analysis*

SPSS (version 26, IBM) was used for statistical analyses of plant growth and phytohormone content. All data were subjected to independent sample T-testing, and the statistical results were expressed as mean ± standard error (MSE). Correlations were calculated using the Pearson's correlation analysis method. Statistical significance was established at $P \leq 0.05$.

## Results

*Root morphology of plants grown at different flow rates*

To measure the effects of the nutrient solution flow rate on root growth and development, we observed the phenotypic characteristics of the entire plant at F0 (0 L/min), F7 (7 L/min), and F14 (14 L/min; Fig. 2A). As depicted in Fig. 2B–G, the fresh weight of the shoot and root, total root length, root surface area, root volume, and average root diameter of plants differed significantly under different flow rates. Shoot and root fresh weights significantly increased with an increased flow rate (Fig. 2B, C). The total root lengths of F7 and F14 increased by 15.1 % and 28.5 %, respectively, compared to F0 (Fig. 2D), and the root surface area increased by 16.4 % and 42.1 %, respectively (Fig. 2E). The root volume and average root diameter of the plants also significantly increased with the flow rate: compared to F0, the root volumes and average root diameters of F7 and F14 increased by 18.3 % and 3.1 % and 57.5 % and 10.7 %, respectively (Fig. 2F and 2G).

*Hormone levels of plant roots grown at different flow rates*

We measured the indole acetic acid (IAA), ABA, ACC, and jasmonic acid (JA) contents of plant roots grown under three different flow rates. The IAA, ABA, and ACC contents increased with an increased flow rate (3A–3C). Specifically, the IAA content of F14 increased by 57.4 % and 26.7 % compared to F0 and F7, respectively, but there was no significant difference between F7 and F0 (Fig. 3A). In addition, there was no significant difference in the ACC content between F0 and F7 (Fig. 3C), but that of F14 increased by 20.9 % and 13.6 % compared to F0 and F7, respectively. However, the ABA contents of F0, F7, and F14 differed significantly: those of F7 and F14 increased by 69.4 % and 168.7 %, respectively, compared to F0 (Fig. 3B). As the flow rate increased, the JA content initially increased and then decreased. The JA content of F7 and F14 increased by 36.0 % and 16.4 %, respectively, compared to F0 (Fig. 3D). The Pearson correlation coefficient and *P*-value (Fig. 3E) were calculated to determine the relationship between total root length, root surface area, root volume, average root diameter, and hormone content. The correlation between root morphology, IAA, and ABA content were the highest, followed by the correlation between root morphology and ACC, at a significant level.

*RNA-seq analysis and DEGs identified under different flow rates of the nutrient solution*

A transcriptome analysis was conducted on 12 root samples grown at three flow rates (F0, F7, and F14). After data filtering, the number of clean reads ranged from 46,113,650 to 54,726,710, with an average of 49,333,783 for each library. Over 94.6 % of the clean reads had quality scores at the Q30 level, and the GC content ranged from 43.04 % to 43.27 %. Table S2 presents a summary of the RNA-seq data. Of the clean reads, 47,627,501 were mapped to the lettuce genome, with 46,173,355 uniquely mapped. The mapping ratio to the reference genome ranged from 96.32 % to 96.73 %, and the percentage of multiple mapped reads was $<$ 2.97 % (Table S3). The sequencing results were of a relatively high quality and suitable for subsequent analyses.

To identify the key factors in transcriptome data, we used principal component analysis (PCA) to demonstrate changes under different treatments. PCA showed a significant declustering of the three sample groups (Fig. 4A). To identify DEGs significantly enriched in the roots under different flow treatments, we compared the expressions of F0, F7, and F14. After combining all DEGs from the three comparison groups, 1792 DEGs were identified. A hierarchical clustering heat map was created to visualize the expression patterns of all DEGs (Fig. 4B), and a Venn diagram was used to illustrate the number of common and unique DEGs among the three comparison groups (Fig. 4C). In the comparison F7 and F0 comparison group, 730 DEGs were identified, with 195 upregulated and 535 downregulated genes (Fig. 4D); in the F14 and F0 comparison group, 1237 DEGs were identified, with 536 genes upregulated and 701 downregulated (Fig. 4E); and in the F14 and F7 comparison group, 430 genes were upregulated, and 304 were downregulated (Fig. 4F).

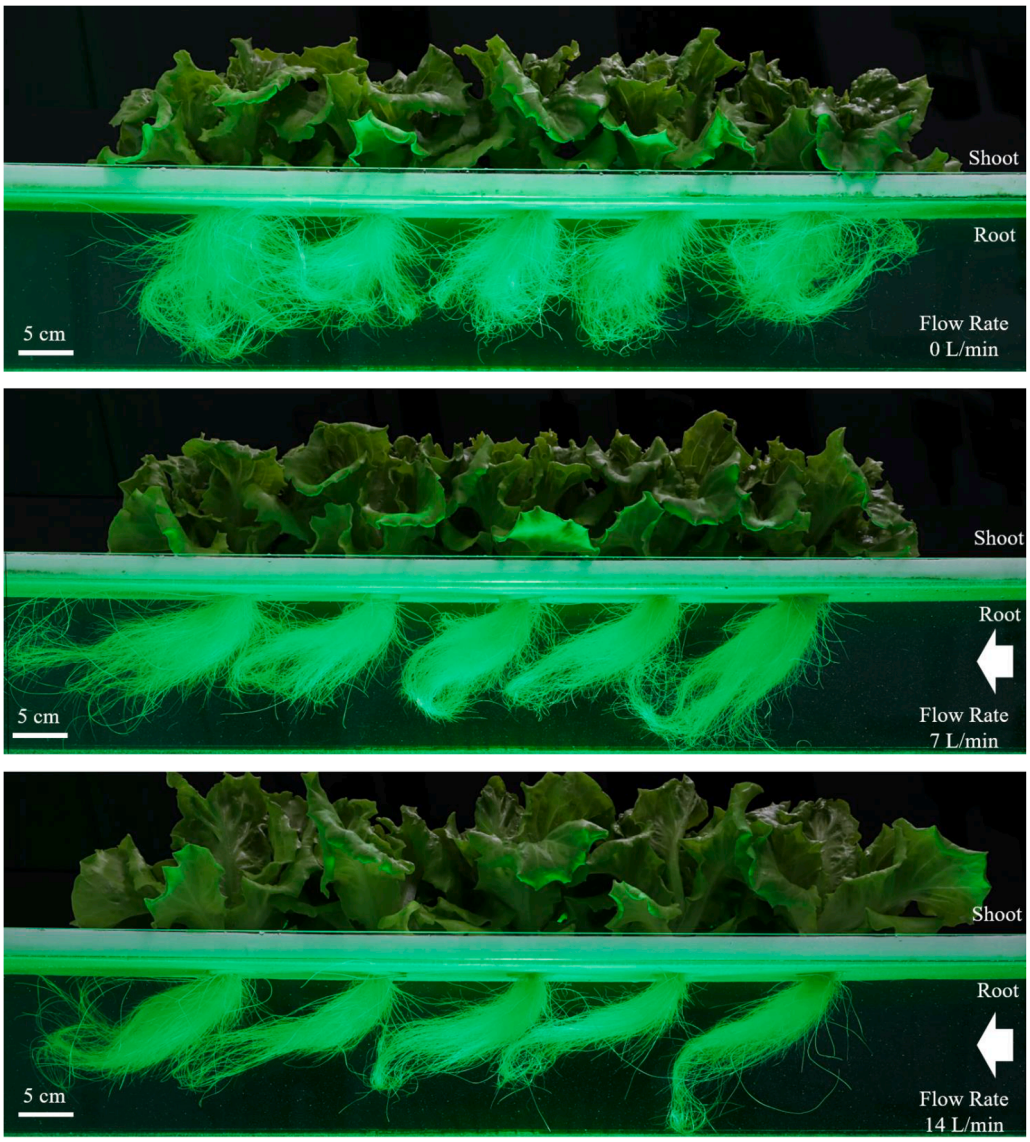


A

**Fig. 2.** Plant growth and root morphology under different flow rate conditions. (A) Plant growth after planting on day 14 (before sampling). (B) shoot fresh weight, (C) root fresh weight, (D) total root length, (E) root surface area, (F) root volume, and (G) average root diameter. Data are expressed as MSE, $n = 10-13$. Statistical significance was analyzed using independent sample T-testing. * $P \leq 0.05$, ** $P \leq 0.01$, *** $P \leq 0.001$, ns: no significant difference.

*GO and KEGG analysis of DEGs*

To identify the biological pathways responding to different flow rates, we mapped all 1792 DEGs to the reference canonical pathways in the KEGG database. Fig. 5A shows the top 20 pathways enriched in DEGs, including the top seven KEGG pathways (phenylpropanoid biosynthesis, biosynthesis of secondary metabolites, MAPK signaling pathway plant, starch and sucrose metabolism, metabolic pathways, stilbenoid, diarylheptanoid, and gingerol biosynthesis, and plant hormone signal transduction).

To explain the biological functions of genes differentially expressed under different flow rate treatments, we conducted a GO enrichment analysis on the 1792 DEGs from the three comparison groups. All DEGs were annotated in the GO database and categorized into three groups (biological process (BP), cellular component (CC), and molecular function (MF)). The GO terms that showed significant enrichment were mainly related to hydrolase activity, which involves the hydrolysis of O-glycosyl compounds (MF), oxidoreductase activity that acts on peroxide as an acceptor (MF), and the catabolic process of peroxidase activity (MF). Furthermore, the terms hydrogen peroxide (BP), apoplast (CC), plant-type cell wall (CC), cell wall (CC), and external encapsulating structure (CC) were also included (Fig. 5B).

*Analysis of DEGs involved in IAA, ABA, and ETH, and JA synthesis and signal transduction*

*DEGs related to IAA synthesis and signal transduction*

Hormones play a crucial role in the growth and development of plants. In this study, we analyzed metabolic pathways (IAA, ABA, ETH, and JA) to explore their impact on the morphological composition of lettuce roots. The results indicated that the gene LOC111918948 (*IAA6*) encoding auxin-induced protein IAA6 was downregulated in F14 (compared to F0) in IAA synthesis and signal transduction (Fig. 6). Furthermore, the gene LOC111910911 (*AUX22D*) encoding auxin-induced protein 22D was downregulated in F7 (compared to F0). There was no significant difference between the other two comparison

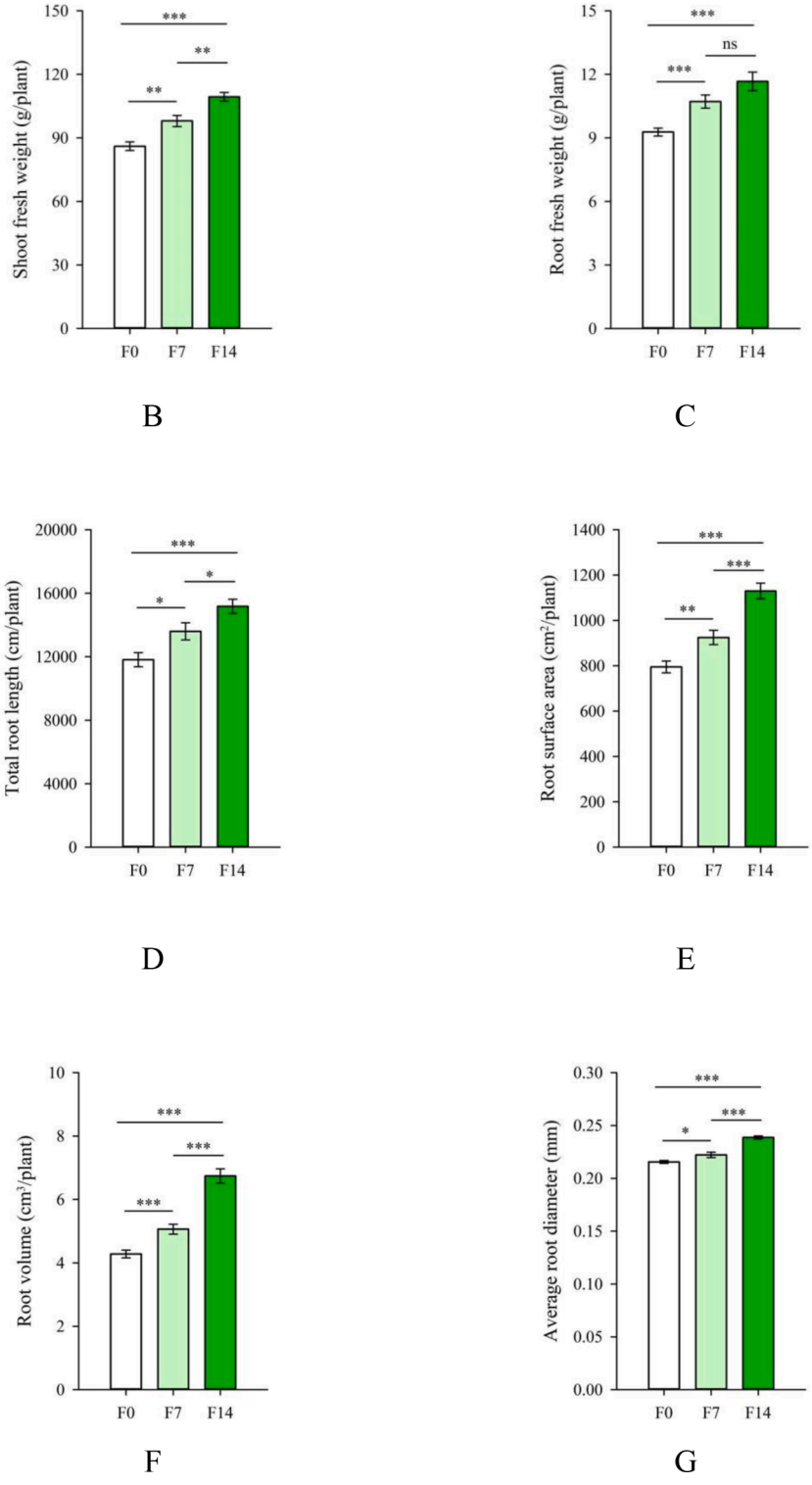


**Fig. 2.** (*continued*).

groups. The gene LOC111918644, encoding auxin response factor 19, was only significantly upregulated in F14, whereas LOC111896378, encoding the auxin response protein GH3 like protein 1, was significantly downregulated compared to F7. Two genes encoding SAUR (LOC111903753 and LOC111917045) showed different trends. LOC111903753 was significantly downregulated in the F7 vs. F0 and F14 vs. F0 comparison groups, but LOC111917045 was only significantly upregulated in the F14 vs. F7 comparison group, and there no significant difference between the other two comparison groups. Significant differences were observed in the levels of metabolites (including tryptophan, tryptamine, and indole) under different flow treatments. Compared to F0, the tryptophan, indole, and auxins contents significantly increased in F7 and F14; however, that of tryptamine significantly decreased. Furthermore, the indole-3-acetamide content was significantly higher in the F7 treatment than in the other two treatments.

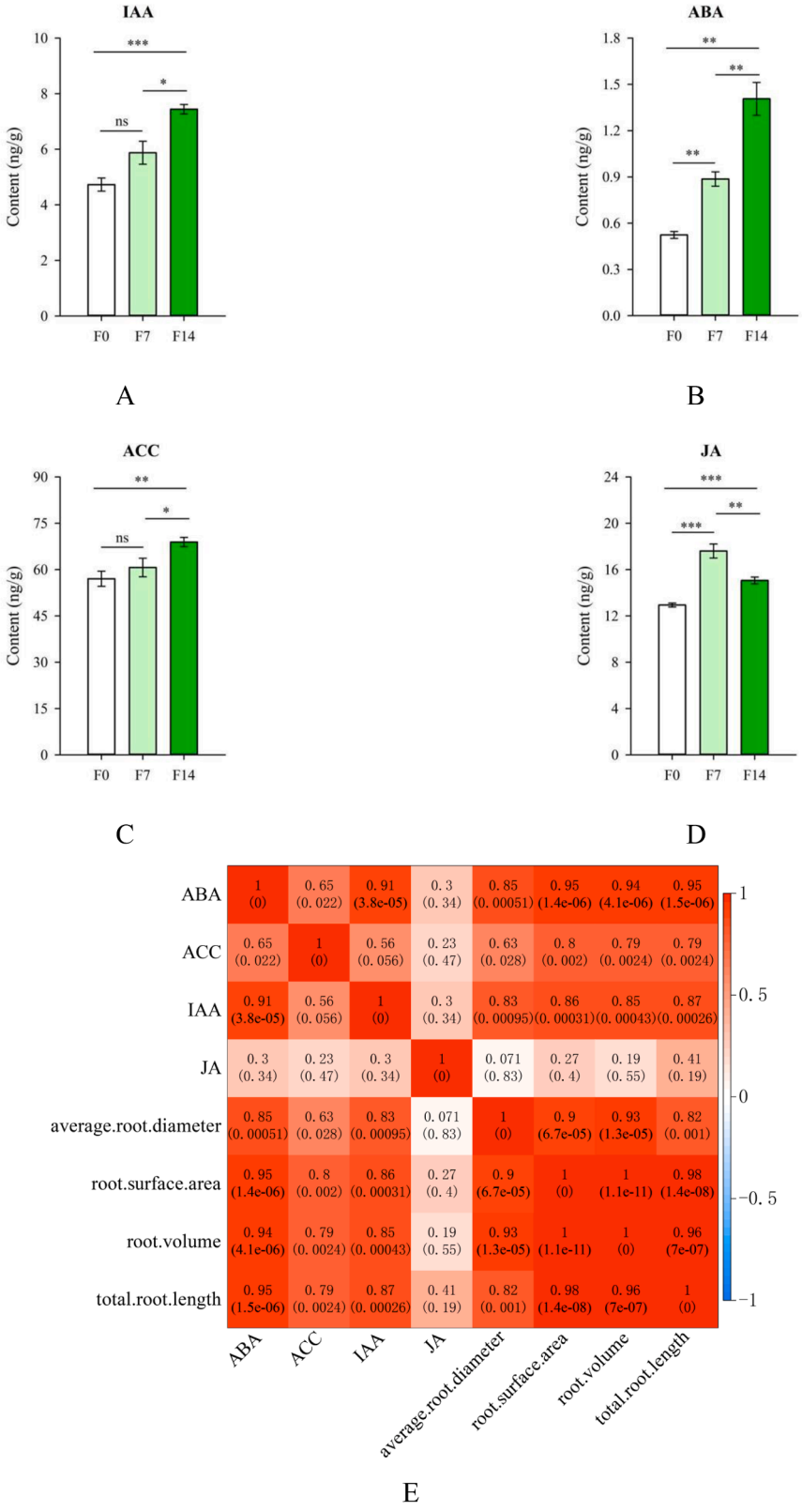


**Fig. 3.** Plant hormone levels in roots under different flow conditions and their correlation with root morphology. (A) auxin (IAA), (B) abscisic acid (ABA), (C) 1-aminocyclopropane-1-carboxylic acid (ACC), (D) jasmonic acid (JA), and (E) correlation between plant hormones and root morphology. Data are expressed as MSE, $n = 4$. Statistical significance was analyzed using independent sample T-testing. * $P \leq 0.05$, ** $P \leq 0.01$, ***$P \leq 0.001$, ns: no significant difference. Correlation was calculated using the Pearson's correlation analysis method.

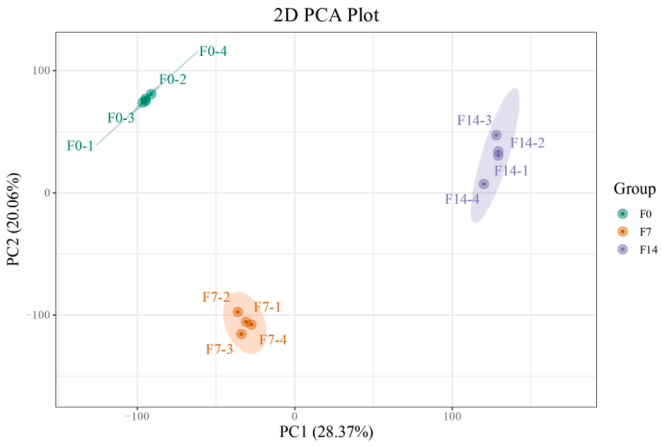


A

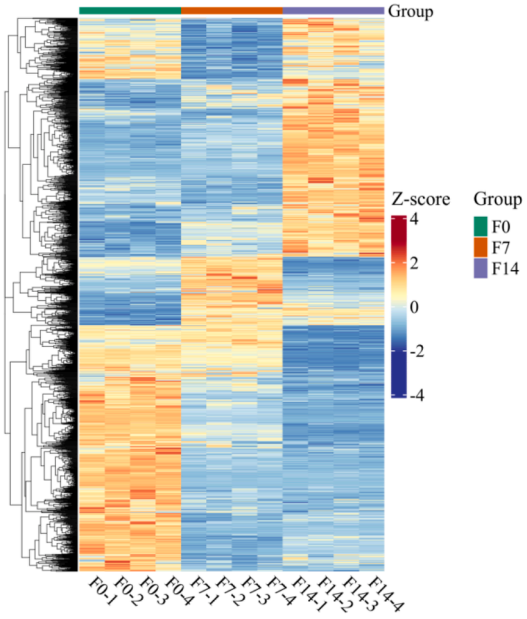


B

**Fig. 4.** PCA, hierarchical clustering heat map, Venn map, and volcano map of the transcriptome. (A) PCA, (B) hierarchical clustering heat map of DEGs, (C) Venn map, (D) volcano map of F7 vs. F0, (E) volcano map of F14 vs. F0, and (F) volcano map of F14 vs. F7.

*DEGs related to ABA synthesis and signal transduction*

Fig. 7 shows that most genes involved in ABA synthesis and signal transduction pathways were upregulated in the F14 vs. F0 and F14 vs. F7 comparison groups. For instance, the genes LOC111912461 encoding LeNCED1, LOC111897148 encoding abscisic aldehyde oxidase, LOC111904052 encoding PP2C, and genes encoding the ABA receptor PYR/PYL (LOC111914132, LOC111914133, LOC111914134) were significantly upregulated in the F14 vs. F0 and F14 vs. F7 comparisons. Although no significant difference was observed between F7 and F0, a difference was observed in F0 and F14 compared to F7. Some genes showed different trends. For instance, LOC111885481, which encodes xanthoxin dehydrogenase, was significantly upregulated in F7 compared to F0 and significantly downregulated in F14 compared to F7. LOC111885488 was significantly downregulated in both F14 vs. F0 and F14 vs. F7. The genes LOC111903643 and LOC111919686, which encode PP2C, were downregulated in F7 vs. F0 and F14 vs. F0. Furthermore, the ABA content was the lowest in F0 and the highest in F14.

*DEGs related to ETH synthesis and signal transduction*

In the ETH synthesis and signal transduction pathways, most genes were downregulated in the F7 and F14 vs. F0 comparisons (Fig. 8). Specifically, the genes encoding ACC synthase 3 (LOC111910693 and LOC111912966), ACC oxidase 1 (LOC111905714), and ethylene receptor 2 (ETR; LOC111897216) were significantly downregulated in F7 and F14 compared to F0. Furthermore, the gene encoding S-adenosylmethionine synthase 2 (LOC111880479) was significantly upregulated in all three comparison groups. In F7, compared to F0, the gene LOC111878569 encoding ACC synthase was upregulated. In F14, compared to F7, LOC111900308 encoding ACC synthase 3 was upregulated. In addition, LOC111893348 encoding serine/threonine protein kinase CTR1 was upregulated in F14 compared to F0. The ACC content was the highest in F14 and the lowest in F0.

*DEGs related to JA synthesis and signal transduction*

Fig. 9 shows that in the JA synthesis and signal transduction pathways, the gene LOC111894364, which encodes phospholipase A2-alpha,

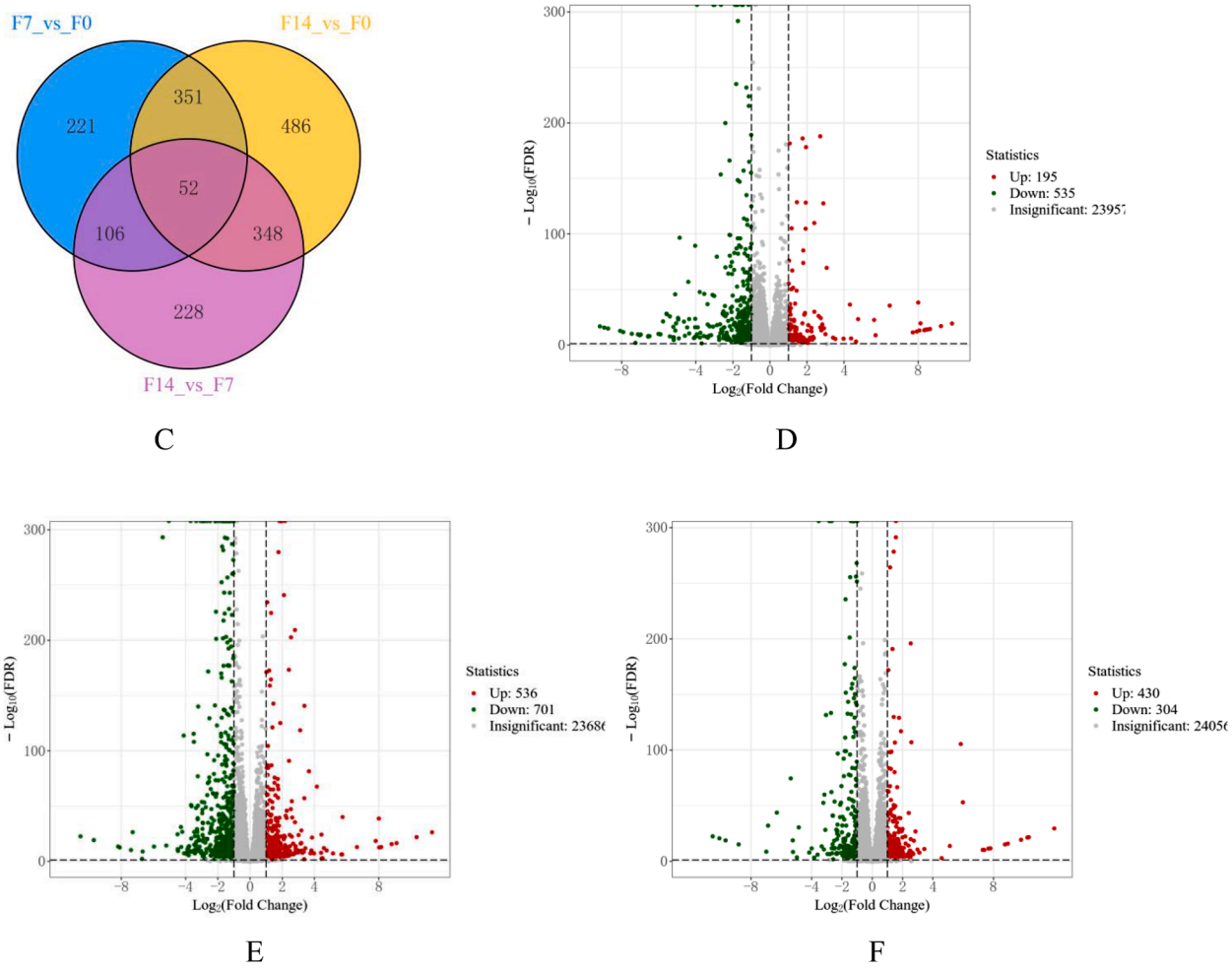


**Fig. 4.** (*continued*).

was significantly downregulated in the F7 vs. F0 and F14 vs. F0 comparisons. Furthermore, the gene LOC111876859, which encodes lecithin-cholesterol acyltransferase-like 1, was downregulated in the F14 vs. F0 comparison. In F14 vs. F0, the gene LOC111911104, which encodes the probable CoA ligase CCL5, was significantly upregulated. Moreover, the gene novel.1250 (*MFP2*), which encodes AtMPF2, was significantly upregulated in the F7 vs. F0 and F14 vs. F0 comparisons. Compared to F0, the genes LOC111877445 and LOC111907574, which encode the transcription factor bHLH, exhibited a downregulated expression trend in F7 and F14. Conversely, the other two genes encoding the transcription factor MYC2 (LOC111896842 and LOC111906387) were significantly upregulated in F14 (compared to F0). In addition, as the flow rate of the nutrient solution increased, the contents of JA and jasmonoyl-L-isoleucine (JA Ile) showed an initial increase followed by a decrease.

### *Correlation network analysis*

Fig. 10A shows the correlation network analysis between DEGs in the four hormone biosynthesis and signal transduction pathways (Tables S4−S13). Out of the 43 DEGs, 21 exhibited a positive correlation with indole-3-acetic acid (IAA). The top 10 DEGs with the highest correlation coefficients were LOC111907488 (*P2C24*), LOC111918644 (*ARF19*), LOC111897148 (*AAO3*), LOC111911104 (*CCL5*), LOC111914133 (*RAP*), LOC111880479 (*METK2*), LOC111904052 (*AHG1*), LOC111912461 (*NCED1*), LOC111906387 (*BHLH25*), and LOC111914132 (*RAP*) ($r > 0.8$). Among the 22 DEGs negatively correlated with IAA, those with the highest correlation were LOC111883974 (*SRK2E*), LOC111879857 (*PYL4*), LOC111885488 (*ABA2*), and LOC111919686 (*PYL4*). Among the 43 DEGs, those positively correlated with ABA included LOC111914133 (*RAP*), LOC111918644 (*ARF19*), LOC111914132 (*RAP*), LOC111897148 (*AAO3*), LOC111907488 (*P2C24*), LOC111880479 (*METK2*), LOC111904052 (*AHG1*), and LOC111912461 (*NCED1*). Those negatively correlated with ABA included LOC111879857 (*PYL4*), LOC111883974 (*SRK2E*), LOC111885488 (*ABA2*), LOC111919686 (*PYL4*), LOC111910693 (*ACS3*), and LOC111877445 (*BHLH93*). Among the 22 DEGs positively correlated with ACC, those with a higher correlation primarily included LOC111914132 (*RAP*), LOC111880479 (*METK2*), LOC111897148 (*AAO3*), and LOC111914133 (*RAP*). DEGs negatively correlated with ACC included LOC111885488 (*ABA2*), LOC111879857 (*PYL4*), LOC111883974 (*SRK2E*), and LOC111896378 (*GH3.1*). DEGs positively correlated with JA included novel genes 1250 (*MFP2*) and LOC111887871 (*LOX2.1; P* $\leq$ 0.05); DEGs negatively correlated with JA included LOC111903753 (*SAUR12*), LOC111897216 (*ETR2*), LOC111910911 (*AUX22D*), and LOC111903643 (*RAP*).

Fig. 10B shows the correlation network analysis between the DEGs in the biosynthesis and signal transduction pathways of the four hormones. Eighteen pairs of genes showed a positive correlation between DEGs in the IAA synthesis and transduction pathways and DEGs in the ABA synthesis and transduction pathways, whereas 11 pairs exhibited a negative correlation. Furthermore, 10 gene pairs were positively correlated and one pair negatively correlated between DEGs in the IAA synthesis and transduction pathways and DEGs in the ETH synthesis and

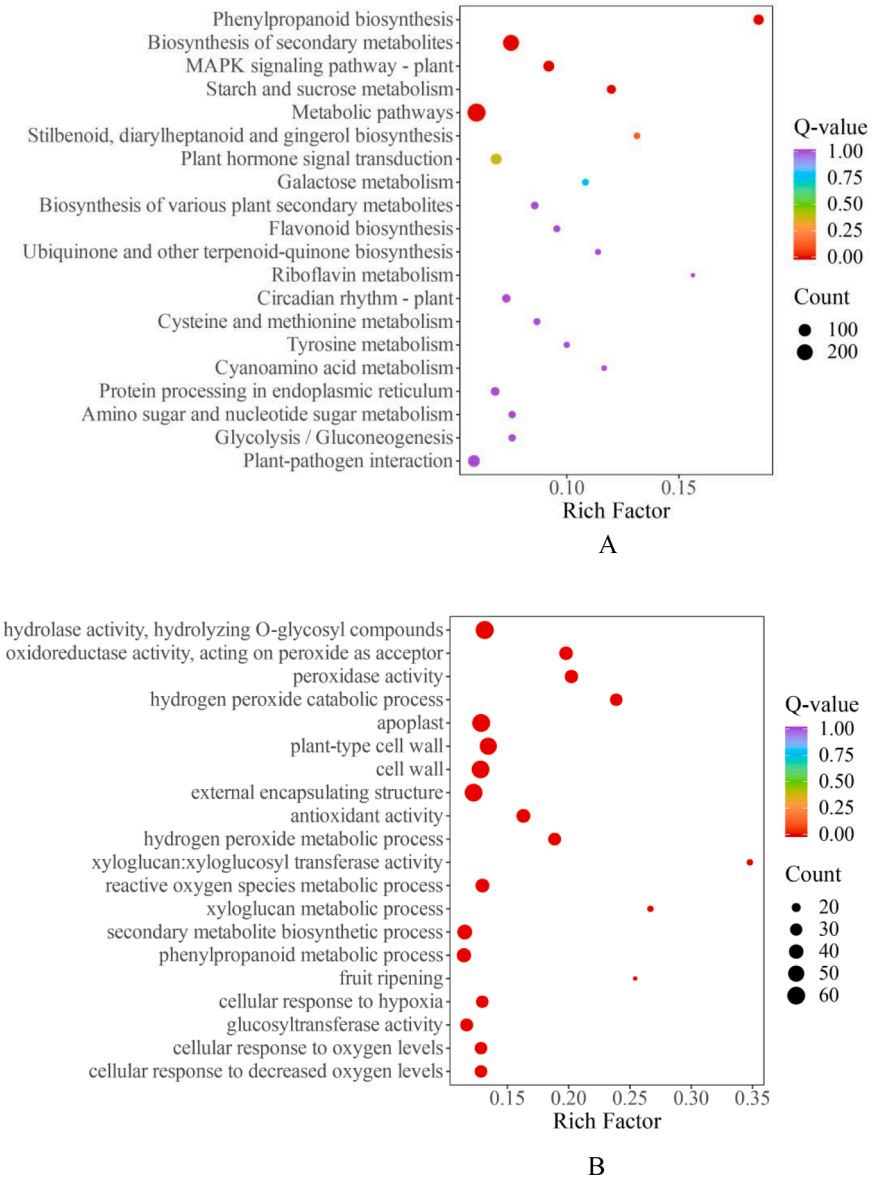


**Fig. 5.** Enrichment map of KEGG pathways and GO terms in different treatment groups. (A) Enrichment map of KEGG pathways and (B) enrichment map of GO terms.

transduction pathways. Positive correlations were observed between eight gene pairs in the IAA synthesis and transduction pathways and three in the JA synthesis and transduction pathways. Moreover, 32 gene pairs showed positive correlations and 13 negative correlations between DEGs in the ABA synthesis and transduction pathways and DEGs in the ETH synthesis and transduction pathways. Twenty-two genes were positively correlated and 13 negatively correlated between the DEGs in the ABA synthesis and transduction pathways and the DEGs in the JA synthesis and transduction pathways. In addition, 10 gene pairs showed a positive correlation between the DEGs in the ETH synthesis and transduction pathway, and 9 gene pairs showed a negative correlation.

*Real-time qRT-PCR analysis*

To validate the transcripts, we selected 16 genes from the plant hormone metabolism pathways for qRT-PCR analysis. The results showed that the expression trends of target genes were largely similar to those of the transcriptome analysis (Fig. 11). The qRT-PCR results showed that among these 16 genes, the relative expression levels of five genes increased with an increase in the nutrient solution flow rate. For example, *METK2, AAO3*, and *P2C24* genes had the lowest mRNA levels under the F0 treatment and the highest under the F14 treatment. The relative expression levels of seven genes decreased with increasing nutrient flow, including *PYL4, SRK2E*, and *ABA2* genes, which had the highest mRNA levels under the F0 treatment and the lowest under the F14 treatment. qRT-PCR suggested that varying nutrient flow rates significantly affected the root morphology and the genes associated with hormone metabolism.

## Discussion

*Effects of nutrient solution flow rate on root morphology and plant growth*

The hydroponic nutrient solution flow field is the liquid flow environment in which plant roots grow. As such, it comprises the physical and chemical properties of the liquid and the hydrodynamic forces acting on the roots. In hydroponics, plant root morphology is directly affected by the flow environment of the nutrient solution, and it influences the root distribution and growth direction. For example, the root system experiences fluid resistance and shear forces during growth

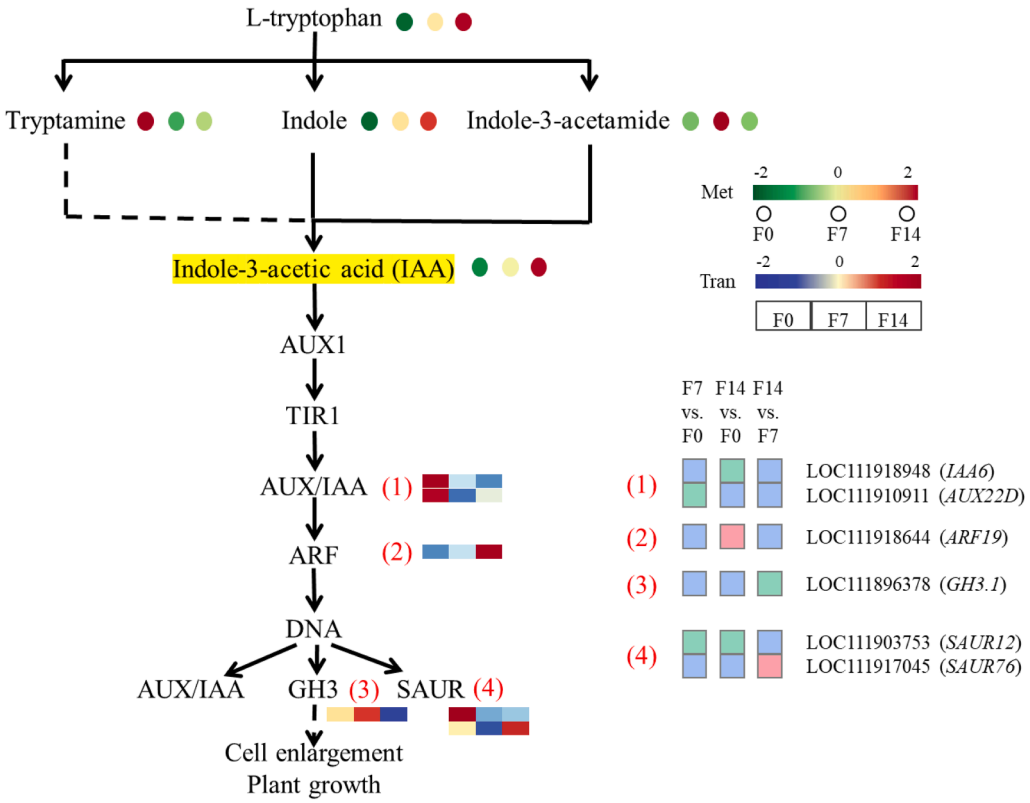


**Fig. 6.** Metabolites and DEGs involved in IAA synthesis and signal transduction.

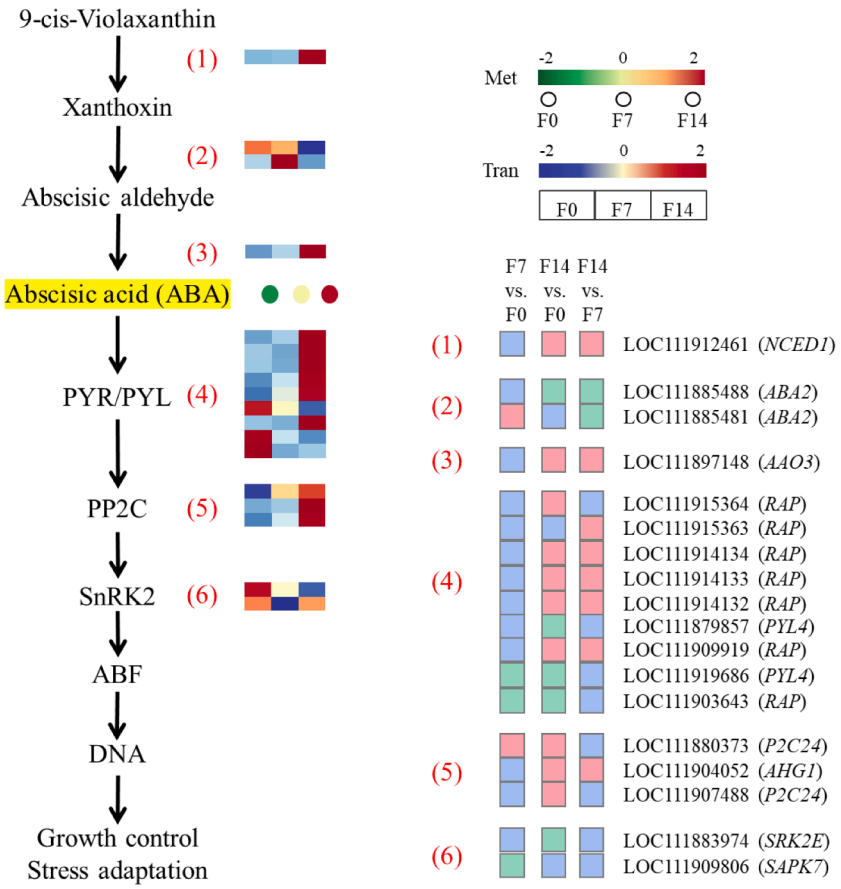


**Fig. 7.** Metabolites and DEGs involved in ABA synthesis and signal transduction.

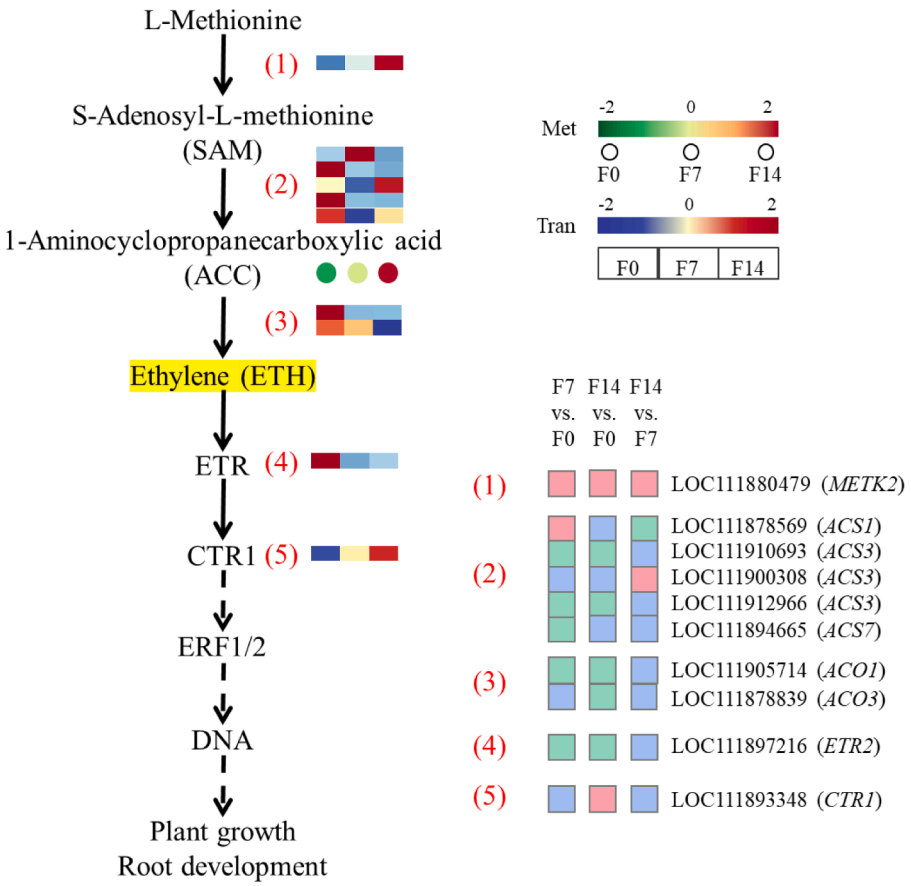


**Fig. 8.** Metabolites and DEGs involved in ETH synthesis and signal transduction.

that can affect extension (Baiyin et al., 2021a). In an appropriate flow environment, hydrodynamic forces can stimulate root growth by applying mechanical stimuli to plant roots (Baiyin et al., 2021c). This study examined the impact of the nutrient solution flow rate on root growth by analyzing the impact of nutrient flow on plant root morphology and growth and exploring the underlying mechanisms.

The results showed that root length, surface area, volume, and average diameter increased with flow rates within a suitable range. Compared to stagnant water, adequate flow rates promoted root growth. Furthermore, a positive correlation was observed between plant hormone levels and root morphology. A strong correlation exists between auxin and ABA, root length, and other indicators. Fluid environments can affect the metabolic activity of plant roots by regulating their growth and biological functions through hormones; such effects are primarily generated by fluid dynamics, mechanical stimulation, and chemical regulation. Therefore, understanding and controlling the impact of the flow environment on plant root morphology and growth is important for optimizing plant growth and development and improving crop yield and quality.

This study revealed that the fresh weight of the edible shoot increased with a higher nutrient solution flow rate, suggesting that compared to static nutrient solution conditions, flowing nutrient solutions promote rapid growth of the entire plant. Therefore, regulating the flow of nutrient solutions in hydroponic plant factories is crucial for accelerating plant growth. Hydroponic nutrient solutions are an effective means of providing plants with the necessary nutrients, and regulating the flow environment of the nutrient solution can promote sufficient contact between the roots and nutrient ions, thereby increasing nutrient absorption (Baiyin et al., 2021b), which promotes rapid fulfillment of plant nutritional needs and accelerates their growth rate. Regulating the nutrient flow field environment can accelerate plant growth; this has multiple implications for hydroponic cultivation, and employing such measures can improve the efficiency and quality of hydroponic cultivation production, meet the food needs of urban populations, and promote sustainable agriculture development.

### *Differences in plant hormone synthesis and signal transduction in roots induced by the flow environment*

#### *Auxin*

Auxins are a class of plant hormones that serve multiple functions: they promote cell division and elongation, aid tissue expansion, stimulate plant stem and leaf growth (Woodward and Bartel, 2005), and regulate the direction and speed of root growth (Overvoorde et al., 2010). As such, auxin plays a crucial regulatory role in plant growth and development, affecting plant growth morphology, organ development, and environmental adaptation (Zhao, 2010). Auxin synthesis in plants occurs mainly through multiple enzyme-catalyzed reactions. In this study, relevant metabolites in the IAA synthesis pathway were detected using tryptophan as a substrate. IAA biosynthesis occurs through the tryptophan, indole, and indole-3-acetamide pathways (Fig. 6). There were significant differences in the tryptophan, indole, and indole-3-acetamide contents under different flow rates as intermediate products in the synthesis of IAA (Fig. S1), and the IAA content was affected by the three synthesis pathways. The contents of tryptophan, indole, and indole-3-acetic acid showed similar trends under the flow treatment, suggesting that the main auxin synthesis pathway under flow treatment may be from tryptophan to indole to indole-3-acetic acid.

The AUX/IAA gene family is a crucial component of the auxin signaling pathway in plants, and it comprises multiple members that perform distinct functional roles in plant cells. The encoded protein regulates hormone responses during plant cell growth and development,

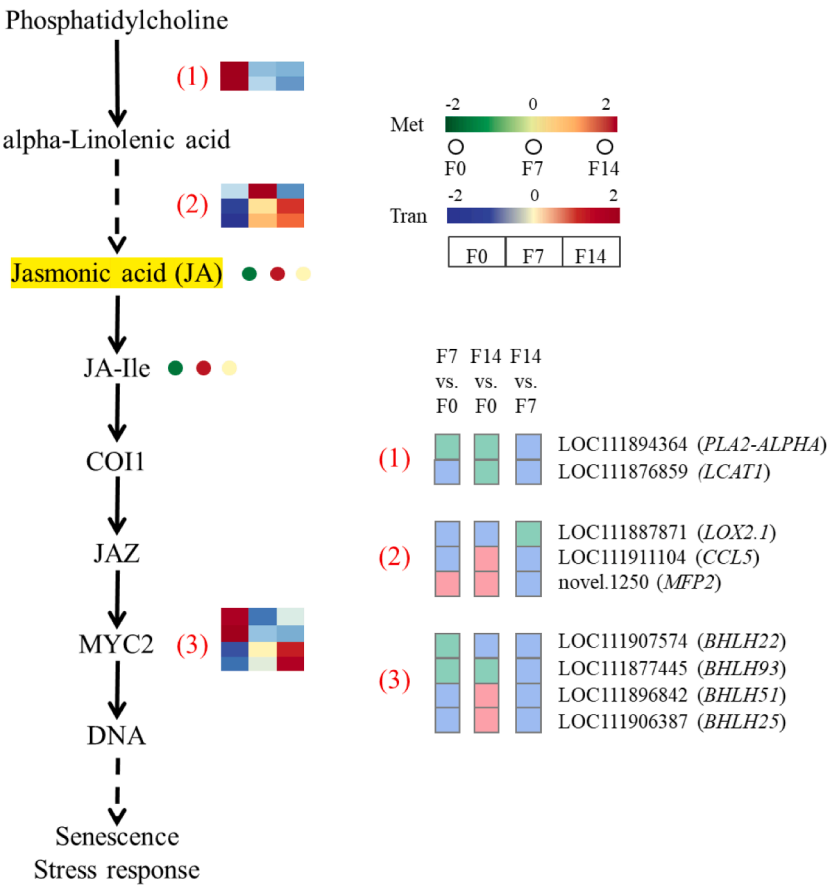


**Fig. 9.** Metabolites and DEGs involved in JA synthesis and signal transduction.

and AUX/IAA genes are responsible for regulating auxin sensitivity in plants. Upon binding to cellular receptors, auxin signals are transmitted to the nucleus, which affects gene transcription and expression. Auxin response factor (ARF) is a transcription factor that binds auxins and regulates the expression of downstream genes; the protein products of the AUX/IAA gene regulate auxin signaling by binding to ARF proteins in the protein family (Liscum and Reed, 2002). Upon binding to the auxin receptor (TIR1/AFB) in the cytoplasm, ARF is activated after translation. In addition, ARF proteins are activated and bind to DNA to regulate downstream gene expression (Calderón Villalobos et al., 2012). Therefore, the ARF gene family is crucial in regulating various aspects of plant growth and development, such as root development, leaf unfolding, and fruit development.

When the auxin concentration is low, the AUX/IAA protein inhibits ARF activity, which inhibits the expression of specific genes. However, as the concentration of auxin increases, AUX/IAA proteins are degraded, ARF factors are released, and specific gene expression is promoted. This regulatory mechanism enables plants to regulate their growth and development based on changes in external hormone concentrations (Lakehal et al., 2019). The auxin concentration was lower under F0, leading to a relatively high expression level of AUX/IAA, which inhibited the expression of ARF. Conversely, under the F7 and F14 conditions, the auxin concentration was higher, resulting in a relatively low expression level of AUX/IAA and promoting the expression of ARF.

During root growth, GH3 plays a crucial role in regulating the metabolism and signaling of plant auxins, and regulation of the GH3 gene can affect root growth rate, root hair formation, and root architecture establishment (Wang et al., 2020a). External environmental signals regulate the expression of the GH3 gene. GH3 family members encode GH3 proteins that act as co-proteins in plant cells, and GH3 proteins can affect plant auxin metabolism and signal transduction by binding to auxin and other signaling molecules (Wang et al., 2023). GH3 catalyzes auxin binding to natural or artificially synthesized amino acids, forming covalent ester conjugates of auxin and amino acids. This esterification reaction is an auxin inactivation pathway in plants, which regulates auxin concentration and activity. GH3 also couples auxin with coenzyme A, forming an aminoacyl coenzyme A-IAA complex and reducing the auxin content in plant cells (Park et al., 2007). Furthermore, GH3 can affect auxin activity and control root growth and development by regulating auxin transport and expressing auxin-related transport proteins (Wojtaczka et al., 2022). Its expression level is relatively high under normal circumstances and can inhibit the expression of auxin transporters.

Limiting auxin transport to specific parts can reduce its overall distribution. This localized regulation of auxin transport is crucial for root growth and allows for the precise control of auxin distribution within the root system. Our findings indicated that the GH3 content was significantly higher under F0 and F7 conditions than under F14, and this increased expression may have inhibited the corresponding effect of auxin. Although GH3 expression may have been influenced by the flow environment under F14 conditions, leading to its inhibition, auxin was not affected by GH3, and its growth-promoting effect was better exerted. This resulted in higher values for root length and surface area indicators than under F0 and F7.

The SAUR gene family plays a crucial regulatory role in root growth and is associated with the auxin signaling pathway. It is widespread in the plant genome and contains multiple structurally similar members that may differ in expression patterns and regulatory functions. The primary function of these members is to regulate the growth and extension of plant cells, promote seedling elongation and root growth, and unfold leaves and flower organs (Du et al., 2020). SAUR's response to auxin in plants is rapid, and its expression levels change substantially

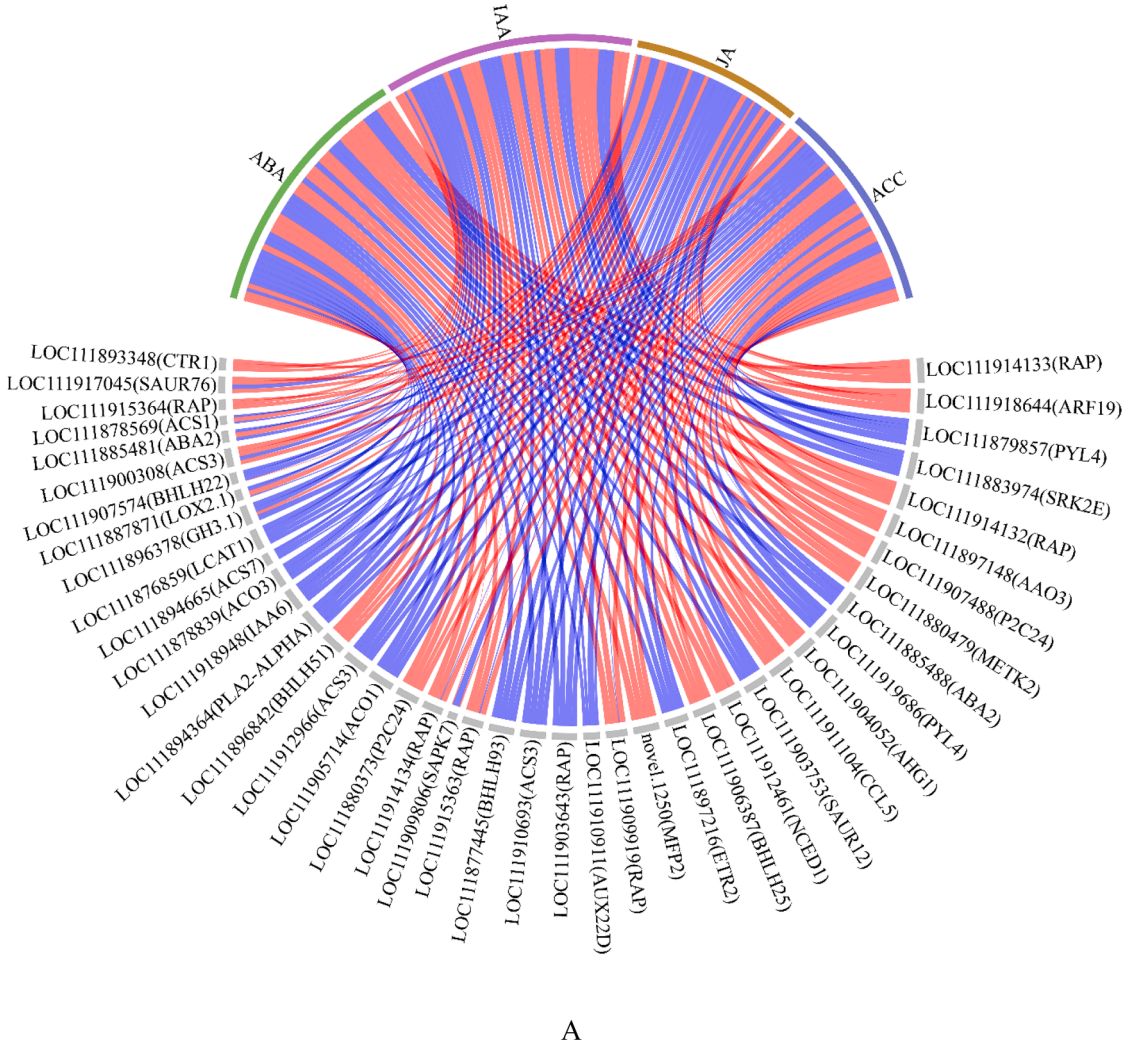


A

**Fig. 10.** Relationship between DEGs and the synthesis and transduction of four phytohormones. (A) Interaction between DEGs and phytohormone synthesis transduction; (B) interaction between DEGs. in (A) the red and blue lines represent positive and negative correlations, respectively, and the thickness of the line indicates the strength of the correlation. In (B) the solid and dashed lines represent positive and negative correlations, respectively. Green lines represent DEGs in ABA synthesis and signal transduction pathways; blue lines represent DEGs in the ethylene synthesis and signal transduction pathways; purple lines represent DEGs in auxin synthesis and signal transduction pathways; and brown lines represent DEGs in the JA synthesis and signal transduction pathways.

over short timescales. SAUR genes encode proteins with stable RNA structures that can be rapidly translated into proteins and regulate auxins through pathways such as cell growth and expansion. SAUR also helps to regulate cell elongation and division during root growth. The expression of SAUR is regulated by auxin, and changes in the auxin concentration can affect its expression level. SAUR expression is also influenced by environmental factors, such as temperature (Ren and Gray, 2015). SAURs are expressed in various developmental stages and plant tissues with spatiotemporal specificity.

The mechanism by which SAUR plays a role in cell growth and extension is not fully understood, but some studies have improved our understanding of its functions. SAUR proteins may be related to cell wall relaxation, which can affect plasticity and stretchability by regulating the activity of cell wall enzymes or cell wall synthesis, promoting cell growth and extension (Du et al., 2020). The protein products of SAUR regulate gene expression related to cell wall relaxation and cell elongation, promoting root cell elongation. In addition, SAUR overexpression or deletion can cause abnormal growth and development in plants, emphasizing its role in regulating plant growth (Wang et al., 2020b).

The expression level of *SAUR12* was higher in the F0 treatment compared to the F7 and F14 treatments, with no significant difference between F7 and F14. The expression level of *SAUR76* was higher in the F14 treatment compared to the F7 treatment, and there were no significant differences in expression levels between the F7 and F0 treatments. The expression levels of these two genes did not consistently increase or decrease with increasing flow rates, and it was thus challenging to identify a unified pattern to explain the impact of the flow rate on their expression levels.

The SAUR gene exhibited a rapid response and changes in expression levels. However, the protein it encodes has a stable RNA structure, and future proteomic studies could confirm the impact of flow on its expression level. The SAUR gene family is a crucial component of the plant genome, and it participates in plant growth and development by regulating cell growth and elongation. Despite the widespread attention SAUR has received in plant biology studies, further research is needed to fully elucidate its function.

*Abscisic acid*

ABA is a crucial endogenous hormone present in plants, and it

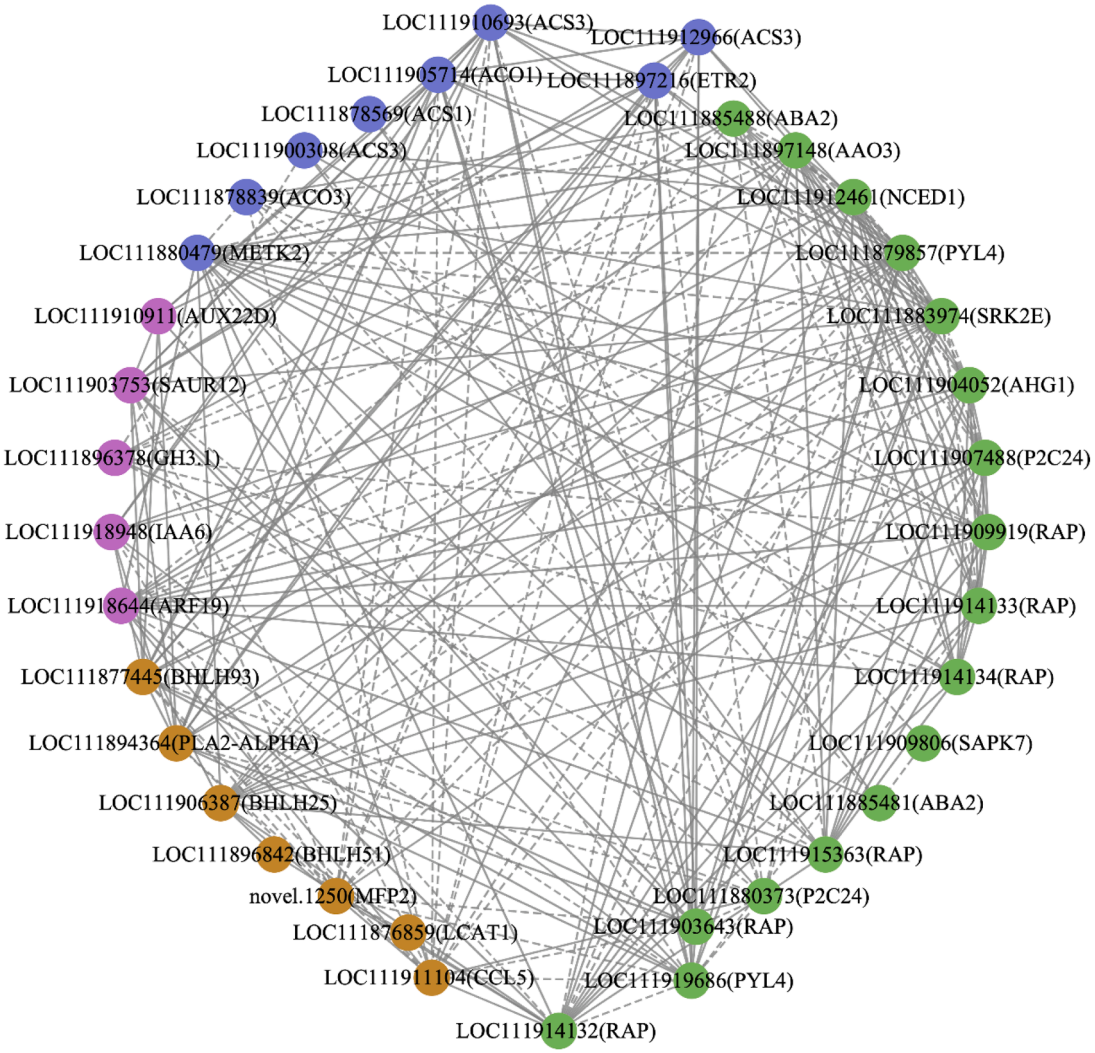


B

**Fig. 10.** (*continued*).

primary functions include regulating seed germination, growth, flowering, and promoting plant adaptation and response to adverse conditions such as drought, high salinity, and low temperatures (Zhang et al., 2006). The biosynthesis of ABA occurs through two main pathways: terpenoid and carotenoid pathways. The carotenoid pathway involves the polymerization of mevalonate (MVA) to form the C40 precursor, carotenoid. This is then cleaved into C15 compounds such as xanthaldehyde (XAN), which is gradually converted to abscisic acid (ABA) through a series of enzymatic reactions involving xanthoxin dehydratase and abscisic aldehyde oxidase. Higher plants synthesize ABA mainly through the carotenoid pathway (Jiang and Hartung, 2008). In this study, metabolites related to ABA synthesis in the carotenoid pathway were detected. The expression level of abscisic aldehyde oxidase was significantly higher under the F14 treatment than under F0 and F7, which may explain the higher level of ABA. The ABA level altered significantly with the flow rate, gradually increasing in the F0, F7, and F14 treatments.

The PYR/PYL gene, also known as AHL, is a member of the gene family found in plant cells that encodes the pyrabactin resistance/pyrabactin-like (PYR/PYL) receptor protein (Fidler et al., 2022). These receptors are crucial in mediating plant responses to the environment, specifically regulating ABA signaling and affecting root growth and development. When plant roots are stimulated, they synthesize and release greater amounts of ABA. ABA hormones bind to PYR/PYL receptors in root cells, triggering physiological responses. This ABA-PYR/PYL signaling pathway enables plant roots to respond rapidly to environmental stress and adapt to their surroundings, and activation of PYR/PYL enhances ABA signaling and inhibits plant root growth. AHL proteins form complexes with ABA when plants are exposed to adverse conditions. This binding induces a conformational change in the PYR/PYL receptor, which activates an intracellular signaling complex comprising the protein phosphatase 2C *(PP2C)* and sucrose non-fermenting 1-related protein kinase 2 (SnRK2) (Soon et al., 2012). The activated SnRK2 further promotes downstream responses of ABA signaling, such as initiating the transcription and protein synthesis of stress-resistant genes and inhibiting plant growth and development.

The expression level of PYL4 was significantly higher under treatment with F0 than under conditions F7 and F14. This indicated that ABA signal transduction was partially inhibited under conditions F7 and F14. PP2C is involved in the negative regulation of ABA signal transduction and was strongly expressed in F7 and F14, inhibiting ABA transduction under these conditions. Both ABA and SNRK2 inhibit growth, and when SNRK2 expression increased at F0, growth decreased. However, the expression of SNRK2 was significantly lower at F7 and F14 compared to

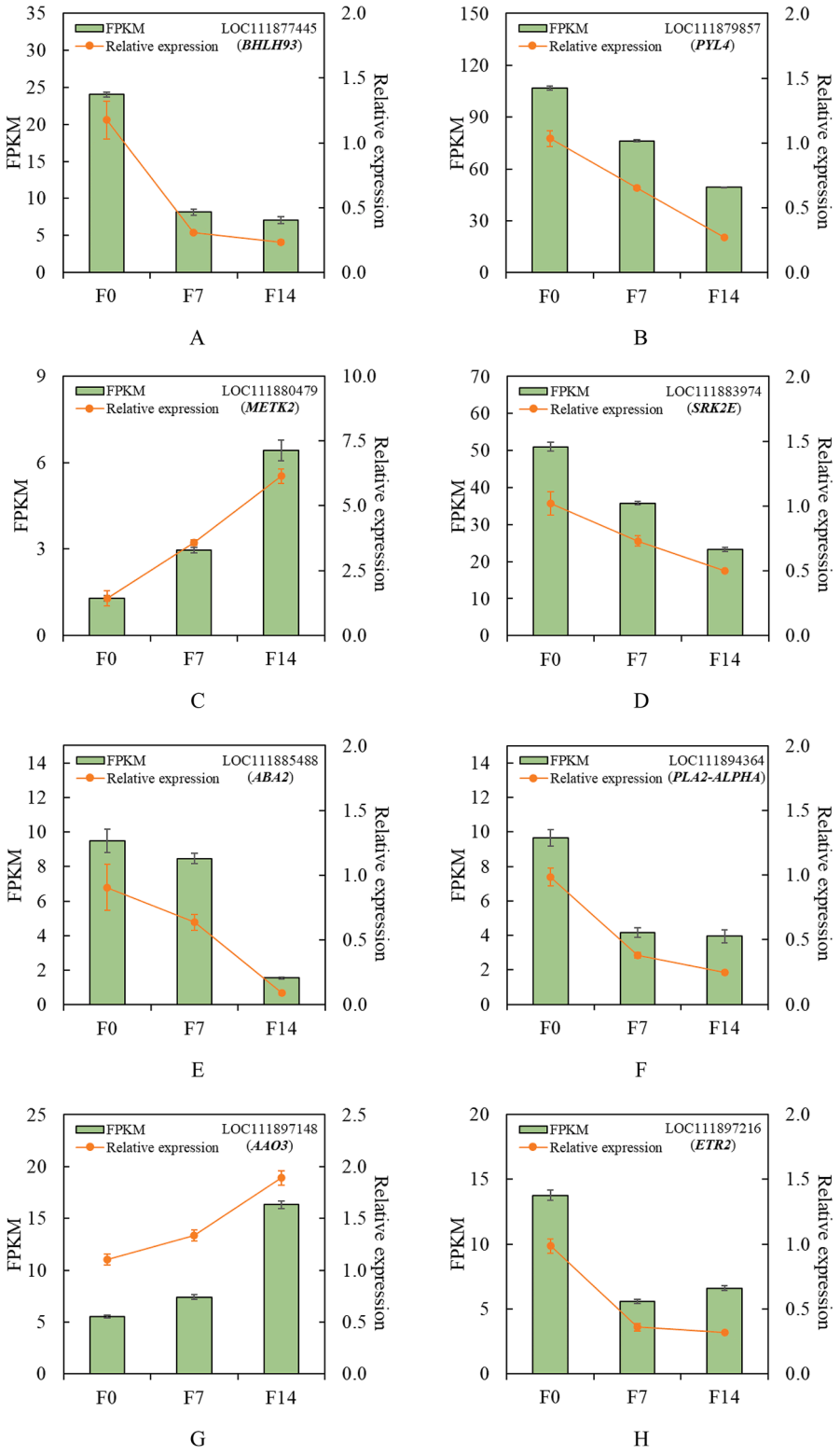


**Fig. 11.** qRT-PCR validation of gene expression levels of 16 selected differentially expressed genes (DEGs) related to hormone metabolism pathways. (A) LOC111877445 (*BHLH93*), (B) LOC111879857 (*PYL4*), (C) LOC111880479 (*METK2*), (D) LOC111883974 (*SRK2E*), (E) LOC111885488 (*ABA2*), (F) LOC111894364 (*PLA2-ALPHA*), (G) LOC111897148 (*AAO3*), (H) LOC111897216 (*ETR2*), (I) LOC111903643 (*RAP*), (J) LOC111903753 (*SAUR12*), (K) LOC111905714 (*ACO1*), (L) LOC111907488 (*P2C24*), (M) LOC111909919 (*RAP*), (N) LOC111910911 (*AUX22D*), (O) LOC111915363 (*RAP*), (P) LOC111919686 (*PYL4*). Data represent the mean and standard error, FPNM, $n = 4$; relative expression, $n = 3$.

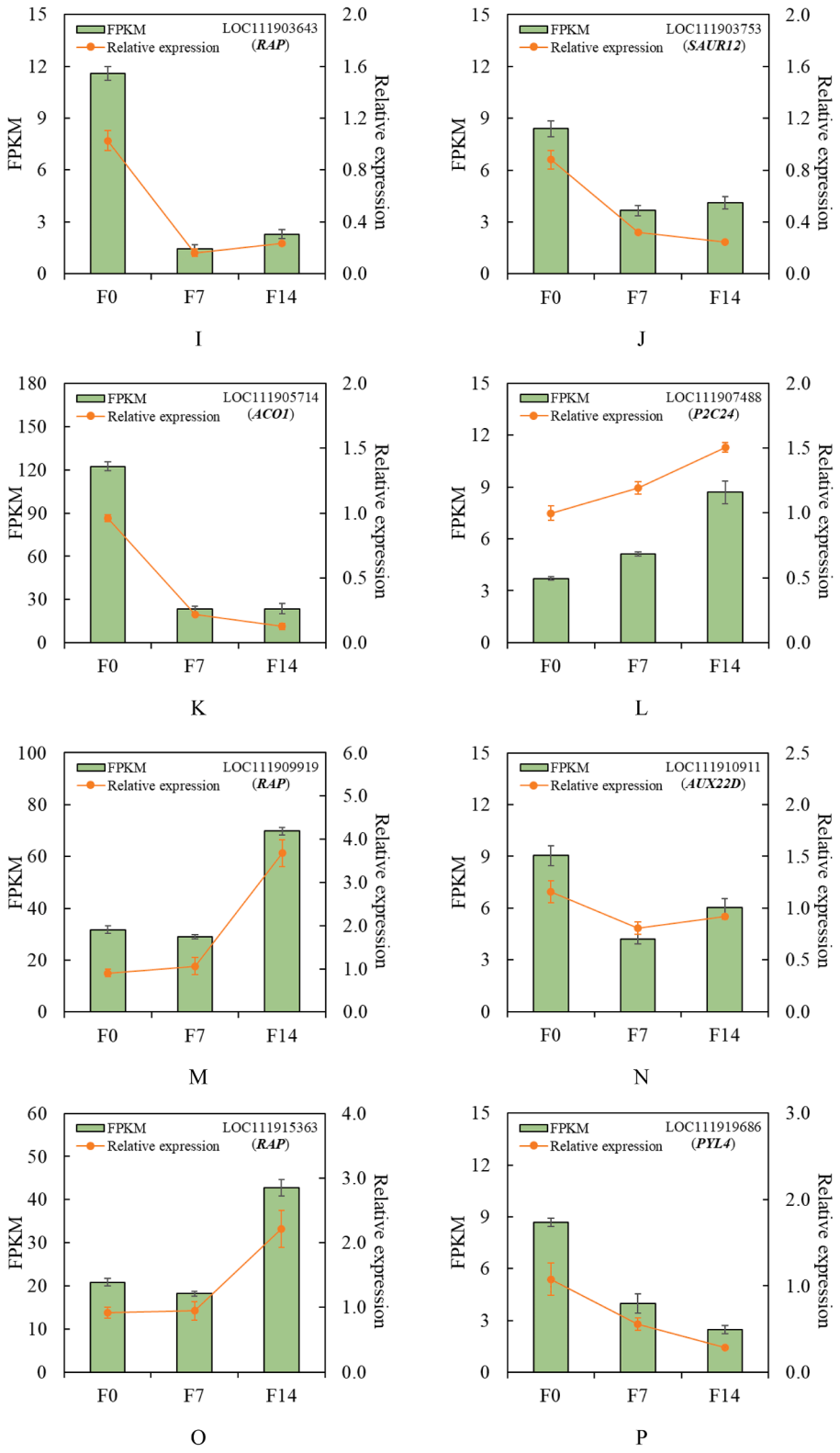


**Fig. 11.** (*continued*).

F0. This suggests that the downregulation of SNRK2 expression counteracted the inhibitory effect of ABA on growth. The experimental results demonstrate that flow induces ABA synthesis, resulting in a higher ABA content under flow conditions than under no-flow conditions. During ABA signal transduction, certain genes that inhibit ABA signal transduction are highly expressed under flow conditions, and these prevent growth-inhibiting ABA from fully exerting its effect. Therefore, the roots of plants growing under flow conditions are no smaller than those growing without flow conditions, but indicators such as root length gradually increase with increasing flow rate.

The RAP gene family is a group of plant genes regulated by ABA signaling. These genes are quickly activated or inhibited by

environmental stress signals such as ABA and polyethylene glycol (PEG), and they play a role in regulating plant adaptation and environmental responses. In the ABA signaling pathway, RAP is gradually activated by ABA signaling. When ABA accumulates in the plant, it forms complexes with specific cellular proteins. The signal transduction of extracellular calcium ions triggers an increase in intracellular calcium ion concentration, which activates corresponding kinases, including $Ca^{2+}$/calmodulin-dependent protein kinases and phosphatases. These enzymes act on a series of downstream signaling pathways, regulating the expression of RAP family genes through specific transcription factors (Chen et al., 2000). The RAP gene is a component of the ABA signaling pathway in plants, and its activation or inhibition affects plant responses to ABA signaling and environmental adaptability. In this study, RAP was highly expressed under conditions F7 and F14, suggesting that it may positively impact plant root adaptation to flowing environments. The RAP gene family could be further studied in practical applications to investigate the molecular mechanisms of plant response to ABA. The results could serve as a foundation for enhancing plant stress resistance and improving crop yield and quality (Liang et al., 2011).

*Ethylene*

Ethylene is a simple unsaturated hydrocarbon compound and an endogenous plant hormone. It is crucial for plant growth, development, fruit ripening, and leaf shedding. It regulates growth processes, such as cell division, elongation, and differentiation, and it promotes cell elongation and relaxation of the cell wall, aiding tissue expansion, growth, and development (Schaller, 2012).

ACC is a precursor molecule in the ethylene synthesis pathway, and it plays a crucial role in this process (Xu and Zhang, 2015). It is an intermediate product of the pathway, and ethylene generation involves the action of two key enzymes, ACC synthase (ACS) and ACC oxidase (ACO). ACS catalyzes the conversion of S-adenosylmethionine (SAM) to ACC, whereas ACO converts ACC to ethylene (Houben and Van de Poel, 2019). ACC is a crucial intermediate in the biosynthesis of ethylene; it is produced in the ethylene biosynthesis pathway, and its accumulation and consumption play essential roles in the regulation and production of ethylene. The ethylene synthases ACS and ACO are regulated by internal and external factors that control the synthesis rate of ACC under normal growth conditions. After ACC is formed, it is converted into ethylene, which regulates various physiological processes such as plant growth, development, fruit ripening, and flowering. In our study, the ACC level gradually increased with the flow rate, whereas the level of ACO decreased with the flow rate. The amount of the ACO enzyme determines the rate of conversion of ACC to ethylene. This alteration could lead to a disparity between variations in the ethylene content with the flow rate and the ACC trend with the flow rate.

ETR is a transmembrane receptor protein that senses and transduces ethylene signals, playing a crucial role in the ethylene signaling pathway. It is the first step in the ethylene sensing and signal transduction pathways, recognizing and bonding ethylene molecules and transmitting signals to downstream components. ETR typically comprises multiple homologous genes that form a gene family. The plant cell membrane contains ETR, which binds to ethylene molecules via its extracellular domain and transmits signals to the cell's interior through signal transduction modules in the intracellular domain (Guo and Ecker, 2004). Ethylene binding to ETR triggers a cascade of ethylene signaling reactions that involve multiple components and regulatory mechanisms to ensure accurate signal transmission and the regulation of downstream physiological processes. When ethylene binds to ETR, it activates a negative regulatory module that reduces the kinase activity of the downstream signaling molecule CTR1 (Constructive Triple Response 1), which typically remains active and inhibits a protein complex that includes the transcription factors EIN2 and E3 ubiquitin ligase. By inhibiting the activity of this complex, CTR1 allows EIN2 to remain stable. When ETR activation negatively regulates CTR1, the kinase activity of CTR1 decreases, inhibiting the EIN2 protein complex. Once this inhibition is released, the EIN2 protein stabilizes and regulates the expression of EIN3 (Shakeel et al., 2015). CTR1 plays a negative regulatory role in the ethylene signal transduction pathway, inhibiting the transduction of the ethylene signal. This regulatory mechanism ensures the precise transmission and regulation of ethylene signals, allowing plants to respond adaptively to external environmental stimuli.

The study revealed that the expression levels of ETR and CTR1 were inversely related. Specifically, ETR expression was upregulated under the F0 treatment but downregulated under the F7 and F14 treatments. Conversely, CTR1 expression was downregulated under the F0 treatment but gradually increased under the F7 and F14 treatments. The F0 treatment resulted in the binding of the highly expressed ETR to ethylene, which inhibited the expression of CTR1 and promoted ethylene signal transduction. In contrast, the low ETR expression under the F14 treatment did not negatively impact the expression of CTR1, which inhibited ethylene signal transduction. ETR, a receptor protein in the ethylene signaling pathway, is crucial for sensing and transducing ethylene hormone signals to downstream components. Plants can adapt to different growth environments and meet the requirements of various physiological processes by regulating the activity and signal transduction of ETR proteins. The flow environment increases the synthesis of the ethylene precursor ACC and affects the expression of related genes such as ACO, ETR, and CTR1, resulting in some inhibition of ethylene signal transduction. The ethylene signaling pathway uses a negative feedback regulatory mechanism to maintain a moderate ethylene response. ETR interacts with and cross-regulates other plant hormone signals, including ABA and auxin; these interactions and cross-regulations make the regulation of environmental changes in plants and their physiological needs more complex and refined.

*Jasmonic acid*

JA is an endogenous hormone found in plants. It plays a crucial role in various physiological processes: JA regulates plant growth and development, flowering time, and root development (Ghorbel et al., 2021), participates in the plant signaling network, interacts with other plant hormones (such as auxin and ABA) to regulate plant growth and response and its most well-known function is in plant defense and stress resistance (Yang et al., 2019).

The α-Linolenic Acid is the starting substance of JA. Galactose oxidase first oxidizes galactose to produce 13-hydroperoxyoctadecatrienoic acid (13-HPOT), a crucial step in JA biosynthesis. 13-HPOT undergoes cyclization via jasmonate ketone synthase (AOS) to produce 12-oxo phosphonic acid (OPDA). OPDA then undergoes carboxylation via JA carboxylase (JMT) to generate JA. Various internal and external factors, such as biological stress, plant pathogen infection, hormone signaling, and environmental stimuli, regulate the biosynthesis of JA, and the regulation of enzyme expression or activity can affect JA production and accumulation (Vick and Zimmerman, 1984).

In this study, JA synthesis was relatively low with no flow treatment but relatively high with flow treatment, indicating that flow promoted JA synthesis. This finding was supported by the expression of LOX-related genes under different treatments. JA glutamyl isoleucine (JA Ile) is a plant hormone that regulates plant growth, development, and resistance to external stresses. The JA pathway is the main biosynthetic pathway of JA, which regulates the expression of certain genes and affects the physiological and biochemical reactions of plants.

The JA signaling pathway is responsible for signal transduction of JA. To bind to its receptors, JA must first be recognized. JA receptors include the coronatine insensitive 1 (COI1) and jasmonate ZIM domain (JAZ) protein families (Ruan et al., 2019). Once JA binds to JA receptors, the JA receptor complex binds to the JAZ protein, leading to its degradation. The JAZ protein acts as a transcription inhibitor that inhibits transcription factors, such as MYC2, through degradation, regulating the expression of downstream genes.

The JA signaling pathway activates transcription factors, such as MYC2, which affect the expression of downstream genes. These genes

participate in JA-induced reactions, including activating defense genes and synthesizing stress-resistant proteins. An important transcription factor in the JA signaling pathway is the basic helix loop helix (BHLH) (Goossens et al., 2017). Certain BHLH transcription factors in the JA signaling pathway are members of the MYC (Myelocytomatosis) family, and they can interact with the JA-responsive factor JAZ, a negative regulator of JA signaling. When JA is present at low levels or is inactive, JAZ can bind to and inhibit the activity of MYC transcription factors. However, when plants are exposed to external stress or the JA signal is activated, the level of JA increases, leading to the degradation of the JAZ protein. This process facilitates the dissociation and activation of MYC transcription factors, promoting the expression of downstream genes that encode defense proteins, synthesize secondary metabolites, and produce other stress resistance-related proteins to enhance plant stress resistance (Boter et al., 2004).

The expression levels of *BHLH22* and *BHLH93* were higher under no-flow conditions and lower under flow conditions. The expression levels of *BHLH51* and *BHLH25* were higher under the F14 conditions than under the F0 conditions. Gene expression within the same family exhibited different trends under the same treatment. The BHLH gene family comprises numerous plant members with diverse functions; certain BHLH genes regulate root growth and differentiation, as well as the formation and function of root hairs (Wang et al., 2020b), and they regulate various plant metabolic pathways, including hormone signaling and secondary metabolite synthesis (Liu and Timko, 2021). The expression of different BHLH genes varies across tissues and developmental stages, and they may perform distinct functions in various physiological processes. Further research on the BHLH gene family is required to deepen our understanding of its diversity and importance in plant biology (Heim et al., 2003).

The JA signaling pathway is a complex network regulated by various factors, such as the cross-regulation of hormone signals, environmental factors, and regulating gene expression. Further research and analysis are needed to fully understand the detailed processes (Ghorbel et al., 2021). A comprehensive study of JA signaling would enhance our understanding of plant growth, development, and stress responses, thus providing a theoretical basis and practical guidance for agriculture and plant physiology research.

### *The interrelationships between hormones and DEGs*

Multiple hormones function together during plant root growth and development. IAA is the main regulatory factor, and it interacts with ABA to regulate root growth. In this respect, *PYL9* in the ABA signaling pathway can enhance the expression of *MYB77*, promoting the interaction between *MYB77* and ARF in the IAA signaling pathway and regulating lateral root growth (Xing et al., 2016). In this study, the levels of gene expression for PYR/PYL and ARF were higher in the F14 treatment compared to the other two treatments, and this greater root growth may have been due to the indirect interaction between these genes. In addition, ABA can regulate the transport and concentration of IAA at specific root sites through the PYR/PP2C/SnRK signaling pathway, indirectly promoting root hair elongation (Zhang et al., 2023). Furthermore, in the study of Guo et al. (2012), PABA inhibited the formation of peanut lateral root primordia by reducing AUX-dependent auxin transport, which is mediated by IAA, and Wang et al. (2011) found that the Arabidopsis ARF2 gene encodes an auxin-responsive factor that can slow the inhibition of ABA on primary root growth.

Ethylene is a crucial plant hormone that regulates root growth, lateral root development, and root orientation. CTR1 is a concentration-dependent inhibitor of IAA biosynthesis that regulates root growth by affecting local IAA biosynthesis (Muday et al., 2012). Ethylene affects plant root growth by affecting TIR1′s perception of IAA (Saini et al., 2013). IAA also upregulates the expression of ACS genes in the ETH synthesis pathway, thus promoting ETH synthesis. In this study, increasing the nutrient solution flow rate upregulated the expression level of the gene LOC111893348 encoding CTR1, which followed the trend of changes in the IAA content. This suggests a potential interaction between ethylene and IAA signaling at different nutrient flow rates, jointly regulating root growth and development. ABA mediates the ethylene pathway and regulates root growth during plant root growth (Luo et al., 2014). ABA induces the phosphorylation of protein kinases *CPK4* and *CPK11*; these phosphorylate ACC synthase (ACS) to maintain protein stability and promote excessive ethylene synthesis, which inhibits root growth (Luo et al., 2014). Under the F0 treatment, the expression levels of *PYL4*, which encodes PYR/PYL, SRK2E, which encodes SnRK2, and *ACS3* and *ACS7*, which encode ACS in the ABA signaling pathway, were higher. Furthermore, the ACC content was the lowest under the F0 treatment, and the ETH content was not detected. Further studies are therefore required to investigate the mutual regulation of ABA and ETH under different flow treatments.

JA and IAA jointly regulate plant growth and development. The exogenous addition of auxin can activate the IAA-TIR-AUX/IAA-ARF signal, which promotes the expression of transcription factor-coding genes, leading to root elongation. This signal also promotes the synthesis of JA, which induces the formation of COI1-JAZ complexes and leads to JAZ degradation, relieving the inhibitory effect of JAZ on MYC2. MYC2 inhibits the expression of genes that encode transcription factors, which regulate root growth (Yang et al., 2019). Root growth was greater in the F7 and F14 treatments than in F0, and this was likely due to the activation of IAA-TIR-AUX/IAA-ARF signals after an increase in IAA content, which promoted root growth. Root growth was greater in the F14 treatment than in the F7 treatment, and this was likely due to the higher JA content in the F7 treatment, which had an inhibitory effect on root growth.

## Conclusion

This study demonstrates that the flow environment of the nutrient solution is a crucial factor in promoting plant growth in hydroponic conditions. The results indicate that the flow of the nutrient solution regulates root morphogenesis by influencing the synthesis and transduction of plant hormone signals, which affects the overall growth of both shoots and roots. During the same growth period, the fresh weight of edible parts of lettuce grown under suitable flow conditions was greater than that of lettuce grown under static flow conditions. This suggests that an appropriate flow rate can promote root growth, leading to overall plant growth. Therefore, suitable flow planting methods can shorten the cultivation period while ensuring the same fresh weight of edible parts or crop yield.

Increasing the flow rate can shorten the cultivation period required. Although this would increase the electricity cost of the water pumps in plant factories compared to static cultivation, it would allow for earlier harvesting, thereby reducing the maximum energy required for lighting and temperature control. This study only analyzed the continuous flow cultivation mode in deep liquid flow cultivation. We suggest that future research should investigate the effects of other cultivation methods (such as pulsating flow and nutrient film technology) on plant root growth, to optimize practical production. In this work, we identified the positive impact of nutrient solution flow mechanisms on plant growth, and our results provide guidance for regulating flow in plant factories to improve yield and save energy.

## Funding

This research was funded by the Agricultural Science and Technology Innovation Program (ASTIP-CAAS).

## CRediT authorship contribution statement

**Bateer Baiyin:** Writing – review & editing, Writing – original draft, Software, Resources, Methodology, Investigation, Funding acquisition,

Formal analysis, Data curation, Conceptualization. **Yue Xiang:** Writing – review & editing, Software, Investigation, Formal analysis, Data curation, Conceptualization. **Yang Shao:** Writing – review & editing. **Jiangtao Hu:** Writing – review & editing. **Jung Eek Son:** Writing – review & editing, Supervision. **Kotaro Tagawa:** Writing – review & editing, Supervision. **Satoshi Yamada:** Writing – review & editing, Supervision. **Qichang Yang:** Writing – review & editing, Supervision, Methodology, Funding acquisition, Conceptualization.

## Declaration of competing interest

The authors declare no conflicts of interest.

## Data availability

Data will be made available on request.

## Acknowledgements

We thank Xinyan Wang for technical support and the Department of Infrastructure Construction of Institute of Urban Agriculture, Chinese Academy of Agricultural Sciences for support at the experimental site.

## Supplementary materials

Supplementary material associated with this article can be found, in the online version, at doi:10.1016/j.stress.2024.100428.

## References

Al-Tawaha, A.R., Al-Karaki, G., Al-Tawaha, A.R., Sirajuddin, S.N., Makhadmeh, I., Wahab, P.E.M., Massadeh, A., 2018. Effect of water flow rate on quantity and quality of lettuce (*Lactuca sativa* L.) in nutrient film technique (NFT) under hydroponics conditions. Bulg. J. Agric. Sci. 24, 791–798.

Baiyin, B., Tagawa, K., Yamada, M., Wang, X., Yamada, S., Shao, Y., An, P., Yamamoto, S., Ibaraki, Y., 2021a. Effect of nutrient solution flow rate on hydroponic plant growth and root morphology. Plants 10, 1840. https://doi.org/10.3390/plants10091840.

Baiyin, B., Tagawa, K., Yamada, M., Wang, X., Yamada, S., Yamamoto, S., Ibaraki, Y., 2021b. Effect of the flow rate on plant growth and flow visualization of nutrient solution in hydroponics. Horticulturae 7, 225. https://doi.org/10.3390/horticulturae7080225.

Baiyin, B., Tagawa, K., Yamada, M., Wang, X., Yamada, S., Yamamoto, S., Ibaraki, Y., 2021c. Effect of substrate flow rate on nutrient uptake and use efficiency in hydroponically grown Swiss chard (*Beta vulgaris* L. ssp. *cicla* 'Seiyou Shirokuki'). Agronomy 11, 2050. https://doi.org/10.3390/agronomy11102050.

Baiyin, B., Tagawa, K., Yamada, M., Wang, X., Yamada, S., Yamamoto, S., Ibaraki, Y., 2021d. Study on plant growth and nutrient uptake under different aeration intensity in hydroponics with the application of particle image velocimetry. Agriculture 11, 1140. https://doi.org/10.3390/agriculture11111140.

Baiyin, B., Xiang, Y., Hu, J., Tagawa, K., Son, J.E., Yamada, S., Yang, Q., 2023. Nutrient solution flowing environment affects metabolite synthesis inducing root thigmomorphogenesis of lettuce (*Lactuca sativa* L.) in hydroponics. Int. J. Mol. Sci. 24, 16616. https://doi.org/10.3390/ijms242316616.

Boter, M., Ruíz-Rivero, O., Abdeen, A., Prat, S., 2004. Conserved MYC transcription factors play a key role in jasmonate signaling both in tomato and Arabidopsis. Genes Dev. 18, 1577–1591. https://doi.org/10.1101/gad.297704.

Calderón Villalobos, L.I.A., Lee, S., De Oliveira, C., Ivetac, A., Brandt, W., Armitage, L., Sheard, L.B., Tan, X., Parry, G., Mao, H., Zheng, N., Napier, R., Kepinski, S., Estelle, M., 2012. A combinatorial TIR1/AFB–Aux/IAA co-receptor system for differential sensing of auxin. Nat. Chem. Biol. 8, 477–485. https://doi.org/10.1038/nchembio.926.

Chen, L., Gao, W., Chen, S., Wang, L., Zou, J., Liu, Y., Wang, H., Chen, Z., Guo, T., 2016. High-resolution QTL mapping for grain appearance traits and co-localization of chalkiness-associated differentially expressed candidate genes in rice. Rice (N Y) 9, 48. https://doi.org/10.1186/s12284-016-0121-6.

Chen, S., Plant, C.C.S., 2000. Regulation by ABA of osmotic-stress-induced changes in protein synthesis in tomato roots. Plant Cell Environ. 23, 51–60. https://doi.org/10.1046/j.1365-3040.2000.00520.x.

Chen, S., Zhou, Y., Chen, Y., Gu, J., 2018. Fastp: an ultra-fast all-in-one FASTQ preprocessor. Bioinformatics 34, i884–i890. https://doi.org/10.1093/bioinformatics/bty560.

Du, M., Spalding, E.P., Gray, W.M., 2020. Rapid auxin-mediated cell expansion. Annu. Rev. Plant Biol. 71, 379–402. https://doi.org/10.1146/annurev-arplant-073019-025907.

Fidler, J., Graska, J., Gietler, M., Nykiel, M., Prabucka, B., Rybarczyk-Płońska, A., Muszyńska, E., Morkunas, I., Labudda, M., 2022. PYR/PYL/RCAR receptors play a vital role in the abscisic-acid-dependent responses of plants to external or internal stimuli. Cells 11 (1352). https://doi.org/10.3390/cells11081352.

Floková, K., Tarkowská, D., Miersch, O., Strnad, M., Wasternack, C., Novák, O., 2014. UHPLC-MS/MS based target profiling of stress-induced phytohormones. Phytochemistry 105, 147–157. https://doi.org/10.1016/j.phytochem.2014.05.015.

Ghorbel, M., Brini, F., Sharma, A., Landi, M., 2021. Role of jasmonic acid in plants: the molecular point of view. Plant Cell Rep. 40, 1471–1494. https://doi.org/10.1007/s00299-021-02687-4.

Gillespie, D.P., Kubota, C., Miller, S.A., 2020. Effects of low pH of hydroponic nutrient solution on plant growth, nutrient uptake, and root rot disease incidence of basil (*Ocimum basilicum* L.). Hortscience 55, 1251–1258. https://doi.org/10.21273/HORTSCI14986-20.

Goossens, J., Mertens, J., Goossens, A., 2017. Role and functioning of bHLH transcription factors in jasmonate signalling. J. Exp. Bot. 68, 1333–1347. https://doi.org/10.1093/jxb/erw440.

Guo, D., Liang, J., Qiao, Y., Yan, Y., Li, L., Dai, Y., 2012. Involvement of G1-to-S transition and AhAUX-dependent auxin transport in abscisic acid-induced inhibition of lateral root primodia initiation in Arachis hypogaea L. J. Plant Physiol. 169, 1102–1111. https://doi.org/10.1016/j.jplph.2012.03.014.

Guo, H., Ecker, J.R., 2004. The ethylene signaling pathway: new insights. Curr. Opin. Plant Biol. 7, 40–49. https://doi.org/10.1016/j.pbi.2003.11.011.

Heim, M.A., Jakoby, M., Werber, M., Martin, C., Weisshaar, B., Bailey, P.C., 2003. The basic helix-loop-helix transcription factor family in plants: a genome-wide study of protein structure and functional diversity. Mol. Biol. Evol. 20, 735–747. https://doi.org/10.1093/molbev/msg088.

Hong, J.H., Seah, S.W., Xu, J., 2013. The root of ABA action in environmental stress response. Plant Cell Rep. 32, 971–983. https://doi.org/10.1007/s00299-013-1439-9.

Houben, M., Van de Poel, B., 2019. 1-aminocyclopropane-1-carboxylic acid oxidase (ACO): the enzyme that makes the plant hormone ethylene. Front. Plant Sci. 10, 695. https://doi.org/10.3389/fpls.2019.00695.

Huang, H., Liu, B., Liu, L., Song, S., 2017. Jasmonate action in plant growth and development. J. Exp. Bot. 68, 1349–1359. https://doi.org/10.1093/jxb/erw495.

Jiang, F., Hartung, W., 2008. Long-distance signalling of abscisic acid (ABA): the factors regulating the intensity of the ABA signal. J. Exp. Bot. 59, 37–43. https://doi.org/10.1093/jxb/erm127.

Kang, H.M., Kim, I.S., 2007. Effect of nutrient solution composition modification on the internal quality of some leaf vegetables in hydroponics. J. Bio-Environ. Control 16, 348–351.

Kim, D., Langmead, B., Salzberg, S.L., 2015. HISAT: a fast spliced aligner with low memory requirements. Nat. Methods 12, 357–360. https://doi.org/10.1038/nmeth.3317.

Lakehal, A., Chaabouni, S., Cavel, E., Le Hir, R., Ranjan, A., Raneshan, Z., Novák, O., Păcurar, D.I., Perrone, I., Jobert, F., Gutierrez, L., Bakò, L., Bellini, C., 2019. A molecular framework for the control of adventitious rooting by TIR1/AFB2-Aux/IAA-dependent auxin signaling in Arabidopsis. Mol. Plant 12, 1499–1514. https://doi.org/10.1016/j.molp.2019.09.001.

Li, Q., Li, X., Tang, B., Gu, M., 2018. Growth responses and root characteristics of lettuce grown in aeroponics, hydroponics, and substrate culture. Horticulturae 4, 35. https://doi.org/10.3390/horticulturae4040035.

Liang, F.S., Ho, W.Q., Crabtree, G.R., 2011. Engineering the ABA plant stress pathway for regulation of induced proximity. Sci. Signal. 4, rs2. https://doi.org/10.1126/scisignal.2001449.

Liao, Y., Smyth, G.K., Shi, W., 2014. Feature Counts: an efficient general purpose program for assigning sequence reads to genomic features. Bioinformatics 30, 923–930. https://doi.org/10.1093/bioinformatics/btt656.

Liscum, E., Reed, J.W., 2002. Genetics of Aux/IAA and ARF action in plant growth and development. Plant Mol. Biol. 49, 387–400. https://doi.org/10.1023/A:1015255030047.

Liu, H., Timko, M.P., 2021. Jasmonic acid signaling and molecular crosstalk with other phytohormones. Int. J. Mol. Sci. 22, 2914. https://doi.org/10.3390/ijms22062914.

Livak, K.J., Schmittgen, T.D., 2001. Analysis of relative gene expression data using real-time quantitative PCR and the $2^{-\Delta\Delta CT}$ method. Methods 25, 402–408. https://doi.org/10.1006/meth.2001.1262.

Love, M.I., Huber, W., Anders, S., 2014. Moderated estimation of fold change and dispersion for RNA-seq data with DESeq2. Genome Biol. 15, 550. https://doi.org/10.1186/s13059-014-0550-8.

Luo, X., Chen, Z., Gao, J., Gong, Z., 2014. Abscisic acid inhibits root growth in Arabidopsis through ethylene biosynthesis. Plant J. 79, 44–55. https://doi.org/10.1111/tpj.12534.

Mir, M.S., Naikoo, N.B., Kanth, R.H., Bahar, F.A., Bhat, M.A., Nazir, A., Mahdi, S.S., Amin, Z., Singh, L., Raja, W., Ahngar, T.A., 2022. Vertical farming: the future of agriculture: a review. J. Pharm. Innov. 11, 1175–1195.

Muday, G.K., Rahman, A., Binder, B.M., 2012. Auxin and ethylene: collaborators or competitors? Trends Plant Sci. 17, 181–195. https://doi.org/10.1016/j.tplants.2012.02.001.

Overvoorde, P., Fukaki, H., Beeckman, T., 2010. Auxin control of root development. Cold Spring Harb. Perspect. Biol. 2, a001537 https://doi.org/10.1101/cshperspect.a001537.

Pacifici, E., Polverari, L., Sabatini, S., 2015. Plant hormone cross-talk: the pivot of root growth. J. Exp. Bot. 66, 1113–1121. https://doi.org/10.1093/jxb/eru534.

Park, J.E., Park, J.Y., Kim, Y.S., Staswick, P.E., Jeon, J., Yun, J., Kim, S.Y., Kim, J., Lee, Y. H., Park, C.M., 2007. GH3-mediated auxin homeostasis links growth regulation with

stress adaptation response in Arabidopsis. J. Biol. Chem. 282, 10036–10046. https://doi.org/10.1074/jbc.M610524200.
Ren, H., Gray, W.M., 2015. SAUR proteins as effectors of hormonal and environmental signals in plant growth. Mol. Plant 8, 1153–1164. https://doi.org/10.1016/j.molp.2015.05.003.
Ruan, J., Zhou, Y., Zhou, M., Yan, J., Khurshid, M., Weng, W., Cheng, J., Zhang, K., 2019. Jasmonic acid signaling pathway in plants. Int. J. Mol. Sci. 20, 2479. https://doi.org/10.3390/ijms20102479.
Saini, S., Sharma, I., Kaur, N., Pati, P.K., 2013. Auxin: a master regulator in plant root development. Plant Cell Rep. 32, 741–757. https://doi.org/10.1007/s00299-013-1430-5.
Sakamoto, M., Suzuki, T., 2020. Effect of nutrient solution concentration on the growth of hydroponic sweet potato. Agronomy 10 (1708). https://doi.org/10.3390/agronomy10111708.
Schaller, G.E., 2012. Ethylene and the regulation of plant development. BMC Biol. 10, 9. https://doi.org/10.1186/1741-7007-10-9.
Shakeel, S.N., Gao, Z., Amir, M., Chen, Y.F., Rai, M.I., Haq, N.U., Schaller, G.E., 2015. Ethylene regulates levels of ethylene receptor/CTR1 signaling complexes in *Arabidopsis thaliana*. J. Biol. Chem. 290, 12415–12424. https://doi.org/10.1074/jbc.M115.652503.
Sheikh, B.A., 2006. Hydroponics: key to sustain agriculture in water stressed and urban environment. Pak. J. Agric. Agric. Eng. Vet. Sci. 22, 53–57.
Šimura, J., Antoniadi, I., Široká, J., Tarkowská, D., Strnad, M., Ljung, K., Novák, O., 2018. Plant hormonomics: multiple phytohormone profiling by targeted metabolomics. Plant Physiol. 177, 476–489. https://doi.org/10.1104/pp.18.00293.
Soares, H.R., Silva, Ê.F., Silva, G.F., Cruz, A.F., Santos Júnior, J.A., Rolim, M.M., 2020. Salinity and flow rates of nutrient solution on cauliflower biometrics in NFT hydroponic system. Rev. Bras. Eng. Agric. Ambient. 24, 258–265. https://doi.org/10.1590/1807-1929/agriambi.v24n4p258-265.
Soon, F.F., Ng, L.M., Zhou, X.E., West, G.M., Kovach, A., Tan, M.H., Suino-Powell, K.M., He, Y., Xu, Y., Chalmers, M.J., Brunzelle, J.S., Zhang, H., Yang, H., Jiang, H., Li, J., Yong, E.L., Cutler, S., Zhu, J.K., Griffin, P.R., Melcher, K., Xu, H.E., 2012. Molecular mimicry regulates ABA signaling by SnRK2 kinases and PP2C phosphatases. Science 335, 85–88. https://doi.org/10.1126/science.1215106.
Thakulla, D., Dunn, B., Hu, B., Goad, C., Maness, N., 2021. Nutrient solution temperature affects growth and Brix parameters of seventeen lettuce cultivars grown in an NFT hydroponic system. Horticulturae 7, 321. https://doi.org/10.3390/horticulturae7090321.
Vandenbussche, F., Vaseva, I., Vissenberg, K., Van Der Straeten, D., 2012. Ethylene in vegetative development: a tale with a riddle. New Phytol. 194, 895–909. https://doi.org/10.1111/j.1469-8137.2012.04100.x.
Vick, B.A., Zimmerman, D.C., 1984. Biosynthesis of jasmonic acid by several plant species. Plant Physiol. 75, 458–461. https://doi.org/10.1104/pp.75.2.458.
Vissenberg, K., Claeijs, N., Balcerowicz, D., Schoenaers, S., 2020. Hormonal regulation of root hair growth and responses to the environment in Arabidopsis. J. Exp. Bot. 71, 2412–2427. https://doi.org/10.1093/jxb/eraa048.
Wang, L., Hua, D., He, J., Duan, Y., Chen, Z., Hong, X., Gong, Z., 2011. Auxin response Factor2 (ARF2) and its regulated homeodomain gene HB33 mediate abscisic acid response in Arabidopsis. PLoS Genet. 7, e1002172 https://doi.org/10.1371/journal.pgen.1002172.
Wang, P., Lu, S., Xie, M., Wu, M., Ding, S., Khaliq, A., Ma, Z., Mao, J., Chen, B., 2020a. Identification and expression analysis of the small auxin-up RNA (SAUR) gene family in apple by inducing of auxin. Gene 750, 144725. https://doi.org/10.1016/j.gene.2020.144725.
Wang, Q., De Gernier, H., Duan, X., Xie, Y., Geelen, D., Hayashi, K.I., Xuan, W., Geisler, M., Ten Tusscher, K., Beeckman, T., Vanneste, S., 2023. GH3-mediated auxin inactivation attenuates multiple stages of lateral root development. New Phytol. 240, 1900–1912. https://doi.org/10.1111/nph.19284.
Wang, T., Wang, S., Wang, Y., Li, J., Yan, F., Liu, Y., Zhao, L., Wang, Q., 2020b. Jasmonic acid–induced inhibition of root growth and leaf senescence is reduced by GmbHLH3, a soybean bHLH transcription factor. Can. J. Plant Sci. 100, 477–487. https://doi.org/10.1139/cjps-2019-0250.
Wojtaczka, P., Ciarkowska, A., Starzynska, E., Ostrowski, M., 2022. The GH3 amidosynthetases family and their role in metabolic crosstalk modulation of plant signaling compounds. Phytochemistry 194, 113039. https://doi.org/10.1016/j.phytochem.2021.113039.
Woodward, A.W., Bartel, B., 2005. Auxin: regulation, action, and interaction. Ann. Bot. 95, 707–735. https://doi.org/10.1093/aob/mci083.
Xiao, H.M., Cai, W.J., Ye, T.T., Ding, J., Feng, Y.Q., 2018. Spatiotemporal profiling of abscisic acid, indoleacetic acid and jasmonic acid in single rice seed during seed germination. Anal. Chim. Acta 1031, 119–127. https://doi.org/10.1016/j.aca.2018.05.055.
Xing, L., Zhao, Y., Gao, J., Xiang, C., Zhu, J.K., 2016. The ABA receptor PYL9 together with PYL8 plays an important role in regulating lateral root growth. Sci. Rep. 6, 27177. https://doi.org/10.1038/srep27177.
Xu, J., Zhang, S., 2015. Ethylene biosynthesis and regulation in plants. In: Wen, C.K. (Ed.), Ethylene in Plants. Springer, Dordecht, pp. 1–25. https://doi.org/10.1007/978-94-017-9484-8_1.
Yang, J., Duan, G., Li, C., Liu, L., Han, G., Zhang, Y., Wang, C., 2019. The crosstalks between jasmonic acid and other plant hormone signaling highlight the involvement of jasmonic acid as a core component in plant response to biotic and abiotic stresses. Front. Plant Sci. 10, 1349. https://doi.org/10.3389/fpls.2019.01349.
Zhang, J., Jia, W., Yang, J., Ismail, A.M., 2006. Role of ABA in integrating plant responses to drought and salt stresses. Field Crops Res. 97, 111–119. https://doi.org/10.1016/j.fcr.2005.08.018.
Zhang, Y., Yang, Zongran, Zhang, Z., Li, Y., Guo, Jinjiao, Liu, L., Wang, C., Fan, H., Wang, B., Han, G., 2023. Root hair development and adaptation to abiotic stress. J. Agric. Food Chem. 71, 9573–9598. https://doi.org/10.1021/acs.jafc.2c07741.
Zhao, Y., 2010. Auxin biosynthesis and its role in plant development. Annu. Rev. Plant Biol. 61, 49–64. https://doi.org/10.1146/annurev-arplant-042809-112308.